Cross Calibration for using Neutron Activation Analysis with Copper Samples to measure D-T Fusion Yields

Chad A. McCoy
May 5, 2011

The University of New Mexico
Department of Physics and Astronomy
Undergraduate Honors Thesis

Advisor:
Gary W. Cooper (UNM ChNE)
Daniel Finley

Abstract

We used a dense plasma focus with maximum neutron yield greater than 10^{12} neutrons per pulse as a D-T neutron source to irradiate samples of copper, praseodymium, silver, and lead, to cross-calibrate the coincidence system for using neutron activation analysis to measure total neutron yields. In doing so, we counted the lead samples using an attached plastic scintillator, due to the short half-life and single gamma decay. The copper samples were counted using two 6" NaI coincidence systems and a 3" NaI coincidence system to determine the total neutron yield. For the copper samples, we used a calibration method which we refer to as the "F factor" to calibrate the system as a whole and used this factor to determine the total neutron yield. We concluded that the most accurate measurement of the D-T fusion neutron yield using copper activation detectors is by using 3 inch diameter copper samples in a 6" NaI coincidence system. This measurement gave the most accurate results relative to the lead probe and reference samples for all the copper samples tested. Furthermore, we found that the total neutron yield as measured with the 3 inch diameter copper samples in the 6" diameter NaI systems is approximately 89 ± 10 % the total neutron yield as measured using the lead, praseodymium and silver detectors.

Table of Contents

Introduction:

Motivation:

The National Ignition Facility (NIF) at Lawrence Livermore National Laboratory is the epicenter for research done in inertial confinement fusion (ICF). At NIF, the research into fusion is being done by laser-driven ICF, powered by the 1.8 MJ ultraviolet laser system with peak power of 500 TW. This system is focused onto a 2 mm diameter pellet, enclosed in a cylindrical gold hohlraum with the pellet filled with a fuel mixture of deuterium and tritium, either as a gas or a thin cryogenic layer [1]. One of the methods used to determine the yield of the pellet implosion is neutron activation analysis. For total neutron yields greater than 10^8, nuclear activation is commonly used due to its ability to accurately measure high neutron yields [2]. In nuclear activation analysis, the high-energy neutrons produced by fusion interact with a material, resulting in the production of an unstable nuclear state with a measurable decay product.

One of the most common materials for neutron activation analysis of D-T fusion neutrons is copper, which due to its high threshold energy, decreases the number of neutrons from other reactions and scattering that could be detected. Both naturally occurring isotopes of copper undergo a (n,2n) reaction resulting in a positron emitter. Upon the annihilation of the positron, this produces two 511 keV gamma rays that can be detected with a coincidence system using two NaI(Tl) detectors. The primary isotope of copper that we are interested in is Cu-63 due to the production of Cu-62 in the reaction $^{63}Cu(n,2n)^{62}Cu$ and the short half-life of 9.74 minutes for Cu-62. This compares to the half-life of 12.7 hours for the Cu-64 produced in the reaction $^{65}Cu(n,2n)^{64}Cu$ [3,4]. As a result of the shorter half-life and greater atom fraction, the activity of the Cu-62 radioisotope will be greater than that of the Cu-64, so the number of counts detected will be more statistically significant above background. On the other hand, the activity of the

Cu-64 would only be marginally significant above the natural background radiation that registers in the detectors. The second reason that the ^{63}Cu(n,2n)^{62}Cu(β^+) reaction is of interest is that all the Cu-62 that is present in the sample comes from that reaction, whereas there is Cu-64 formed by neutron capture in Cu-63[3] along with the Cu-64 from the (n,2n) reaction, thereby complicating the interpretation of the ^{65}Cu(n,2n) ^{64}Cu results.

Theory:

The fusion of deuterium and tritium has been considered the most viable method for achieving ignition since the beginning of research into nuclear fusion. This is because it has the greatest cross section for fusion of most viable fuels, and the cross section peaks at the lowest energy, such that temperatures greater than 4-5 keV can achieve ignition . The fusion of deuterium and tritium results in the production of an alpha particle and a 14.1 MeV neutron[5].

$$d + t \rightarrow {}^4He + n + 17.6 \, MeV$$
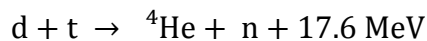
Although fusion is possible at thermal temperatures, to produce a measurable number of fusion neutrons, the energy of the system must be increased. This can be achieved by accelerating particles or adding heat to the overall system. This increase is necessary because the fusion cross section is nonlinear with respect to particle energy with a thermal cross section less than 10^{-4} barns. By accelerating deuterons with an ion beam and directing the beam upon a tritium doped target, such as Erbium tritide, the cross section grows significantly reaching a peak at deuteron energy of 107 keV with the cross section being 4.95 barns[6].

In contrast to the use of deuterium and tritium, the other two commonly used fuel mixtures are far less advantageous for the attempt to reach ignition conditions in nuclear fusion

reactions. These fuel mixtures are pure deuterium, which reacts in a D-D reaction producing either tritium or helium-3, and deuterium and helium-3 which fuse to produce helium-4[7].

$$d + d \rightarrow t + p + 4.03 \text{ MeV}$$

$$d + d \rightarrow {}^3\text{He} + n + 3.27 \text{ MeV}$$

$$d + {}^3\text{He} \rightarrow {}^4\text{He} + p + 18.3 \text{ MeV}$$
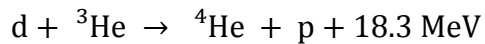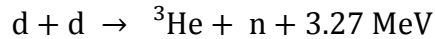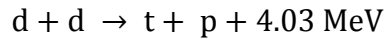
The benefits of these reactions are that the energy output in neutrons is significantly lower than that for D-T and that they do not require a tritium containment system. However, the amount of energy necessary to achieve fusion is significantly higher, and the fusion reaction rate is a fraction of that for D-T. For acceleration using an ion beam, with deuteron energy of 100 keV, the cross sections for both D-D and D-^{3}He fusion are around 20 millibarns, or $1/250^{th}$ the cross section for D-T[6]. As a result, experiments for using these fuels to achieve ignition are non-existent, but the reactions are used to understand the fundamental physics of nuclear fusion and its associated engineering challenges.

The two common methods to irradiate samples with neutrons with energy of 14.1 MeV, such as D-T fusion neutrons, are the use of an ion beam or a dense plasma focus (DPF). Using an ion beam, such as the Sandia Ion Beam Laboratory, generally entails firing a deuteron beam at targets fabricated from a rare earth metal doped with tritium, such as erbium-tritide (ErT_2)[8]. This method is effective because it allows for associated particle counting in the ion beam. Through the use of associated particle counting, a near absolute measurement of the ion flux and total yield can be made. The use of an ion beam also allows for a selection of the deuteron energy with a velocity selector. This allows for the focusing of only those deuterons with approximately optimum energy on the target, rather than having a wide range of deuteron energies and fusion cross sections.

Similar to the use of an ion beam for producing the fusion neutrons necessary for calibration of the (n,2n) reaction in copper, a DPF will act as a neutron source by focusing and heating the plasma in either a z or θ pinch. However, using a DPF to irradiate the sources only allows for a known maximum energy and plasma current due to the construction of the device. As a result, the total yield cannot be calculated directly unless the DPF undergoes a perfect discharge at both maximum energy and plasma current[9].

A DPF works by passing a strong electric current through a plasma, which in turn creates a strong magnetic field that compresses the plasma and locally heats the plasma to fusion temperatures[10]. The Mather-type DPF is designed as a system with two coaxial electrodes, such that by inducing an intense electrical discharge between them, the induced magnetic field in the plasma radially compresses ("pinches") the plasma about the z-axis. This creates a z pinch at the open end, which is treated as a point neutron source, as shown in Figure 1[9].
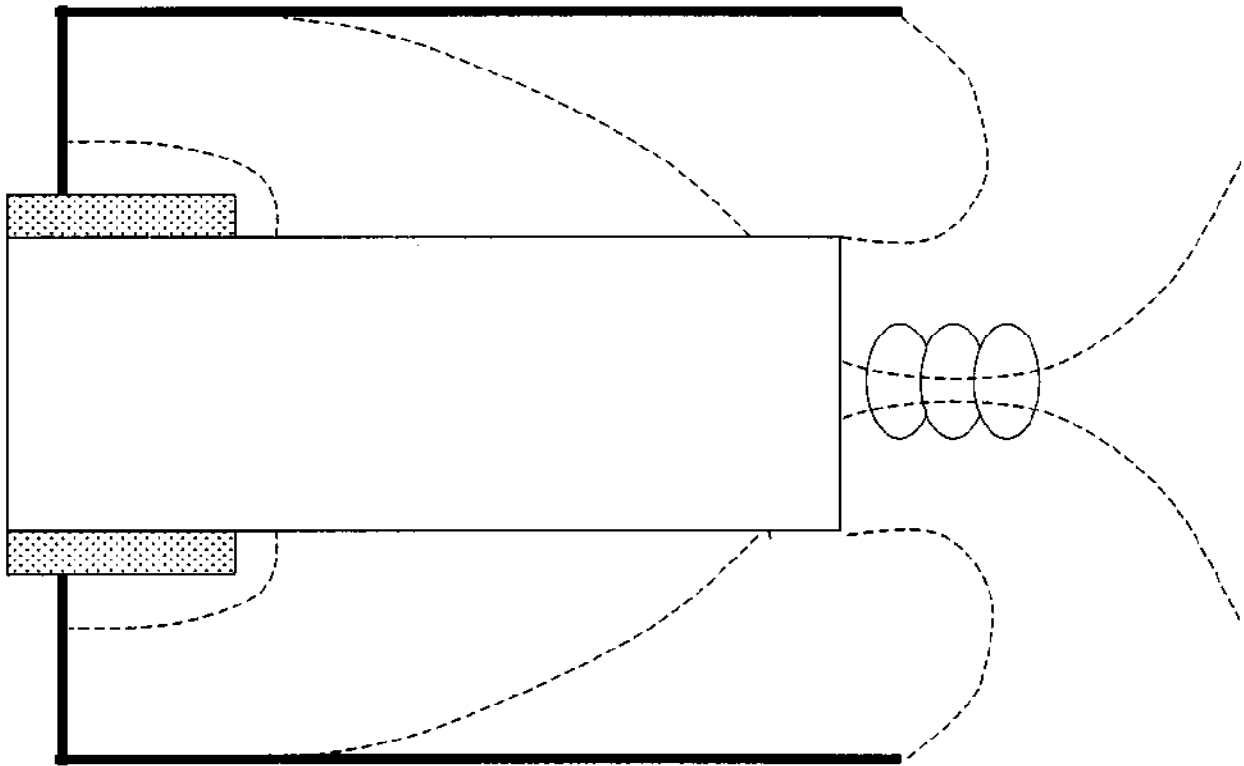
Figure 1: Diagram showing radial compression and formation of z pinch at open end of electrodes in plasma focus[9]

DPF's made with deuterium or D-T plasmas are commonly used as neutron sources due to the relatively uniform heating within the plasma. As this is the case, to achieve D-T fusion, the average particle energy in the pinch needs to be greater than 10 keV due to the nature of the DPF as a pulsed device that rapidly compresses and heats the system. Because a DPF can produce controlled neutron fluxes ranging from the order of 10^4 neutrons per shot to greater than 10^{12} neutrons per shot depending on the size of the device, they are commonly used for neutron activation experiments, along with radiography and other uses if configured to release x-ray pulses. As D-T DPFs are short pulse 14.1 MeV neutron generators, with a pulse lengths ranging from a few nanoseconds to microseconds, they are extremely beneficial in calibration of diagnostics for ICF experiments as they will mimic the neutron output from ICF. The second major benefit in using a DPF for calibration of ICF diagnostics is the required energy for operation, as a DPF will have a significantly higher neutron yield for a given amount of input energy[11].

Neutron activation analysis relies on the reaction between neutrons and atoms of particular isotopes to produce a radioisotope with a known decay sequence. In neutron activation analysis, either the decay of the radioisotope or the emission of a characteristic gamma ray for the transition from a nuclear excited state to ground state is measured, allowing for the determination that a neutron was absorbed by the material[12]. For fusion neutrons, using neutron activation allows for the focusing of a detector on a specific frequency corresponding to the characteristic radiation of the sample material. Neutron activation analysis is also used for determination of material quantities in a mixture based off the measurement of a broad spectrum with peaks corresponding to specific material characteristics. This method can be used for a wide range of neutron energies, including those produced by nuclear fusion.

In using neutron activation for measurements of high-energy neutrons, such as those produced by D-T fusion, it is advantageous to use a material that has threshold energy as close to 14 MeV as possible, provided that the cross section is large enough for significant activation to occur. In doing this, the number of scattered neutrons that interact in the material will be decreased and neutrons produced by most other methods would likely be below threshold. It is also important to use a material that has a relatively short half-life, as a long lived radioisotope will result in a decreased activity and require a longer counting interval. For D-T fusion, the materials that meet these characteristics and are commonly used are copper, lead, indium, and praseodymium. All of these materials have threshold energy for a (n,2n) reaction greater than the neutron energy from the D-D reaction as is given in Table 1. Another material that is being used at NIF is zirconium due to its 12 MeV threshold and high cross section. However, it has a half-life of 3 days and requires a long count time to give results that are statistically significant relative to the background radiation. Sliver is also commonly used for the measurement of neutrons due to its high cross section for neutron capture. However, the threshold energy for silver is very low and it predominantly measures neutrons that have slowed to thermal energies, making it undesirable if other neutron sources are present.

Isotope	Cu-63	Cu-65	In-115	Pr-141	Pb-208
Threshold (MeV)[13]	11.02	10.06	9.120	9.464	7.404
Cross section (mb)[14]	450	910	1470	1440	2220
Daughter Half-life	9.74 min	12.7 h	1.198 min	3.39 min	.80 s

Table 1: Important properties pertaining to neutron (n,2n) reactions in isotopes commonly used for measurement of D-T fusion neutrons

To use a sample for neutron activation analysis and yield determination, the sample needs to be able to have the radioactivity of the product measured. As this is the case, the sample should have a half-life on the order of minutes if it is to be counted outside the target chamber, or be connected to a probe if it has a shorter half-life. For materials that will be counted outside the

target chamber, having positron emitters is advantageous because it allows for the use of two detectors in a coincidence circuit, which in turn allows for the accurate counting of low activities even with large background radiation. The detectors in this case should have the discriminators in the coincidence circuit set for the detection of the characteristic 511 keV gammas that result from electron-positron annihilation. The use of a coincidence circuit for measuring the 511 keV gammas is more effective than using a single detector for materials that have multiple decay products. This is because the discriminators can be set to only measure a window around the 511 keV photo-peak. Then, by knowing the fractional decay rate for positron decay, the total decay rate can be more accurately measured[15]. For the materials given in Table 1, the (n,2n) reaction for Pb-208 results in the meta-stable state of Pb-207, which then emits a single gamma to decay to the ground state of Pb-207[16]. The rest of the materials in Table 1 all undergo positron decay and are effectively counted using a coincidence system to measure the annihilation photons. Silver primarily undergoes β⁻ decay and gamma decay, and is counted with an attached detector similar to that for lead.

The use of copper for the detection of fusion neutrons is beneficial because of its relatively high threshold energy for a (n,2n) capture. Copper is also commonly used because of the short half-life of copper-62, which allows for a distinct calculation of the neutron yield. Also in copper, the resultant isotopes undergo β⁺ emission, such that the 511 keV gammas that are produced by positron annihilation can be measured in a detector with a coincidence system. Because the copper samples are naturally occurring copper, they are comprised of both Cu-63 and Cu-65 with atom percentages of 69.15% and 30.05%, respectively. As there are two distinct radioisotopes that will be produced by (n,2n) reactions in the copper samples, it is important to determine the relative activity of the two isotopes for yield calculations (Eq. 1)[17].

$$A = \lambda N, \qquad \lambda = \frac{\ln(2)}{T_{1/2}} \tag{1}$$

In equation 1, A is the activity of the sample, N is the number of molecules of the radioisotope present in the sample, and $T_{1/2}$ is the half-life of the radioisotope. To determine the relative activity of the Cu-62 and Cu-64, it becomes trivial to take a ratio between the activities of the individual isotopes.

The most common practice used for the modeling of nuclear fusion experiments is the Monte Carlo method. The Monte Carlo method is a statistical process based off the drawing of random samples from specified probability distributions. In Monte Carlo, the samples are drawn as part of a random walk process with the probabilities recalculated after the drawing of each sample and the collection of samples from the random walk building up the probability function. In these samples, the Monte Carlo calculation effectively gives an estimate of the expected value of the estimating random variables. In doing this for neutron transport, the superposition principle allows for Monte Carlo calculations to be run in the different energy regions in a multi-group calculation of neutron energy. This allows for the superposition of solutions to the transport equation for neutrons at different energies and a complete picture of the neutron's interactions without having to use analytical methods[18].

Experiment:

For the experiments at National Security Technologies (NSTec), a Mather-type dense plasma focus with output on the order of 10^{12} neutrons was used. The DPF was mounted in a tritium contaminated pit with a concrete shield over the top, and operated using a deuterium and tritium fuel mixture for producing 14.1 MeV fusion neutrons. The source was aligned with the copper, praseodymium, lead and silver materials in a line of sight for irradiation.

To determine the calibration of the copper system relative to the lead probe, silver detector, and praseodymium samples, it is necessary to calibrate the copper detector system. The calibration of the detector system determines the relationship between the total neutron yield and induced activation in the samples. The methods that could be used to calibrate the detector system are a derivation of the system response with fundamental quantities and the detector efficiency or the "*F* Factor" method developed by G.W. Cooper, C.L. Ruiz, *et. al.*[19] where the entire system is calibrated based off the specific sample geometry, irradiation geometry, and counting geometry. With these quantities modeled into the system, the *F* factor gives a calibration factor for the number of counts recorded per neutron, provided there is knowledge of the number of neutrons incident on the sample. Having done this, the factor can be used for future experiments in the same geometry without the need to know counting efficiencies, cross sections, etc. For the calculations in this experiment, the *F* factor method is used to calibrate the copper detector system for determining total neutron yields from the initial sample activity.

In calibrating the system, there are certain quantities, such as escape probability for gamma rays in the samples, that must be either measured or modeled. For these quantities, modeling was done using MCNPX, which is the Monte Carlo N-Particle eXtended code developed by Los Alamos National Laboratory. This code was used to model the geometries and detector efficiencies given in the system for the determination of the *F* factor and total yield.

After determining the calibration of the detector for the different sizes of copper samples used in the experiment, we compared the calculated yield for each shot to that from the lead probe, silver detector, and praseodymium sample. We chose to use copper samples because the (n,2n) reaction has the highest threshold energy, which results in the detection of the least in-scattering for neutrons, and the material is abundant and relatively inexpensive compared to

praseodymium and other materials. From this, we determined whether the copper samples gave an accurate measurement of the neutron yield or if there was a persistent difference in the measured yield that could imply an error in the calibration method.

Methodology:

F Factor Method[19]*:*

The *F* factor method calibrates the entire system as a unit, rather than determining the calibration factor for the detectors and extrapolating it to the system. This method is beneficial because it eliminates the need to determine the amount of attenuation and scattering that would occur from the specific geometry of the system. This is the case because the geometry is taken into consideration when the *F* factor is measured. As a result, the system is calibrated for that specific geometry and amount of attenuation.

To measure the *F* factor for this experiment, we consider the case where the production of fusion neutrons is approximately steady state. As such, the number of atoms, *N(t)*, of the given radioisotope present at an irradiation time, *t*, can be represented by

$$N(t) = \frac{R\left(1 - e^{-\lambda t}\right)}{\lambda} \tag{2}$$

where *R* is the production rate for the choice radionuclide. As *R* is determined by the parent material and the neutron flux, it can be written in terms of material quantities as

$$R = \frac{\phi \varepsilon_A M N_A \sigma(E)}{A_W} \tag{3}$$

where ϕ is the neutron flux in neutrons/cm^2 s incident on the sample, ε_A is the natural abundance of the parent material in atom fraction, *M* is the mass of the sample, N_A is Avogadro's Number (6.022×10^{23}), A_W is the atomic weight of the material, and $\sigma(E)$ is the cross section for the

neutron capture reaction at energy, E, in square centimeters. With the value of R known, it is possible to calculate the number of atoms of the desired radioisotope at the time when it was removed from the system, denoted as t_0.

With the number of atoms of the desired radioisotope known, the number of counts that would be expected over a time frame in the detector can be determined from the number of atoms present multiplied by the detector's counting efficiency, ε_D, the branching ratio for the desired decay, ε_B, and the proportion of the gamma rays that escape the sample rather than being absorbed, ε_S. Therefore, we can determine that over an interval $t_1 - t_2$, the number of counts, C, including background counts, B, which would be expected, is:

$$C = \frac{\phi \varepsilon_A \varepsilon_D \varepsilon_B \varepsilon_S M N_A \, \sigma(E)}{\lambda \, A_W} \left(1 - e^{-\lambda \, t_0}\right)\left(e^{-\lambda \, t_1} - e^{-\lambda \, t_2}\right) + B \tag{4}$$

If we assume that the number of neutrons emitted is constant, we can define the total neutron yield, Y, as the flux multiplied by the irradiation time times the solid angle, with d the distance from the neutron source to the sample, such that:

$$Y = \phi \, t_0 \, 4\pi d^2 \tag{5}$$

With this yield, we define the calibration factor, F, as:

$$F = \frac{(C - B) t_0 \, 4\pi d^2 \lambda \, A_W}{Y \, M (1 - e^{-\lambda \, t_0})(e^{-\lambda \, t_1} - e^{-\lambda \, t_2})} \tag{6}$$

and from this we get:

$$F = \frac{\varepsilon_A \varepsilon_D \varepsilon_B \varepsilon_S N_A \, \sigma(E)}{A_W} \tag{7}$$

By knowing the F factor, calculations of the total neutron yield become simple. Therefore, to determine the total yield for a short pulse experiment, we can approximate $\left(1 - e^{-\lambda t_0}\right)$ as $\lambda \, t_0$, resulting in the equation for the total yield being:

$$Y = \frac{(C - B)\, 4\pi d^2\, A_W}{F\, M\, (e^{-\lambda\, t_1} - e^{-\lambda\, t_2})} \tag{8}$$

Procedure:

In order to make measurements of the fusion neutrons produced, it is first necessary to set-up and calibrate the detectors and coincidence circuit[20]. As the primary quantity of interest for measurement is the dual 511 keV annihilation photons, it is reasonable to use a detector system that consists of two detectors to measure both photons. Also, because the irradiated source is radioactive and the background counts will be decreased if properly shielded, it is important to have the counting system shielded. Within the counting system, there are two 6" diameter NaI(Tl) detectors located on opposite ends of the lead pig, with the placement of the sample to be counted going in the center of the pig as seen in Figure 2.
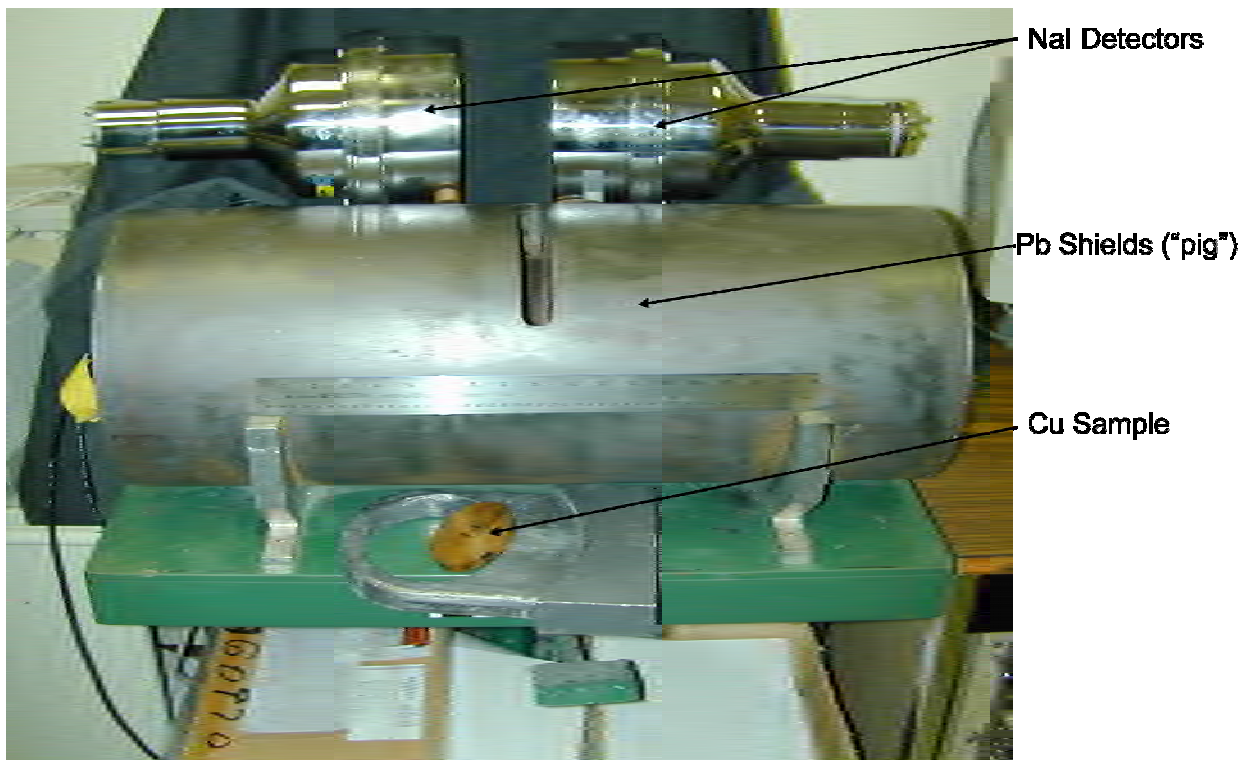
Figure 2: 6" diameter NIF coincidence system for copper activation showing NaI detectors, lead "pig" for shielding, and slot for insertion of copper samples

The data from the detectors is sent through a preamp followed by amplifiers to increase the amplitude of the signal for transmission to the coincidence circuit. The signals are then analyzed using single channel analyzers (SCAs) to select events depositing 511 keV in the NaI scintillator. The SCAs then emit a logic pulse to the coincidence unit, and if a 511 keV event is measured by both SCAs in coincidence an output signal is sent to a multi-channel scaler where the counts were recorded in time bins of 1 minute.
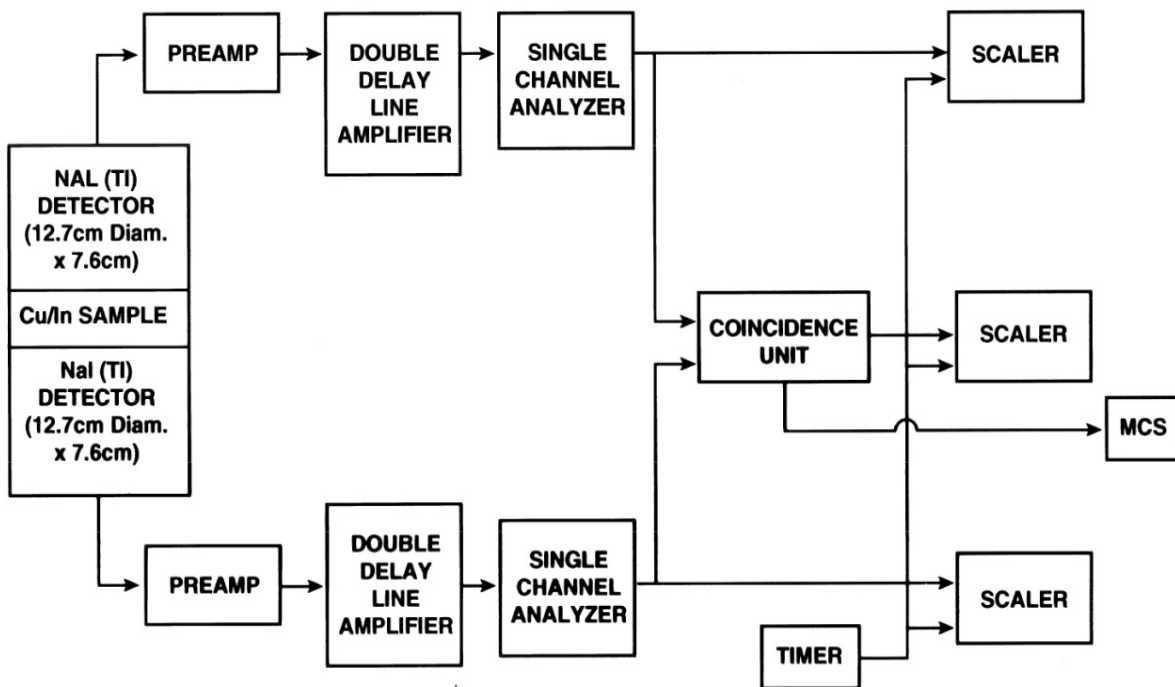
Figure 3: Schematic diagram of coincidence system and electronics for measuring 511 keV photons emitted from positron decay in copper samples

Historically, the system was calibrated using a positron source, such as sodium-22 which undergoes positron decay 90% of the time, but also releases a 1.274 MeV gamma ray 100% of the time. As a result, the higher energy gamma can result in the coincidence system missing counts due to summing events from the 1.274 MeV gammas moving the count outside the discriminator window, resulting in a smaller calculated counting efficiency. This happens because the deposition of energy from the 1.274 MeV gamma at the same time as one of the 511

keV gammas registers in the detector as a single photon with energy 1.785 MeV. If the summing

events are not taken into account, the measurement of the counting efficiency is off by about a

factor of two.   However, by using the *F* factor method, the counting system is calibrated to a

copper sample, such that a Na-22 source is only necessary for setting the coincidence windows

and measuring the detector efficiency. Because the summing events involving the 1.274 MeV

gamma emitted by Na-22 complicates the measurement of the efficiency, we used a Ge-68

source, which has almost no summing events and gives an almost absolute of the detector

efficiency for modeling of the efficiency for copper sources in MCNP.

    To take data at NSTec, the copper samples were attached to a train car, which was in turn

attached to a tape measure, such that the samples were lowered a given length into the chamber

for irradiation as shown in Figure 4. Also noted in Figure 4 are the locations of the lead, silver,

and praseodymium as all the samples were irradiated at the same time for each shot.
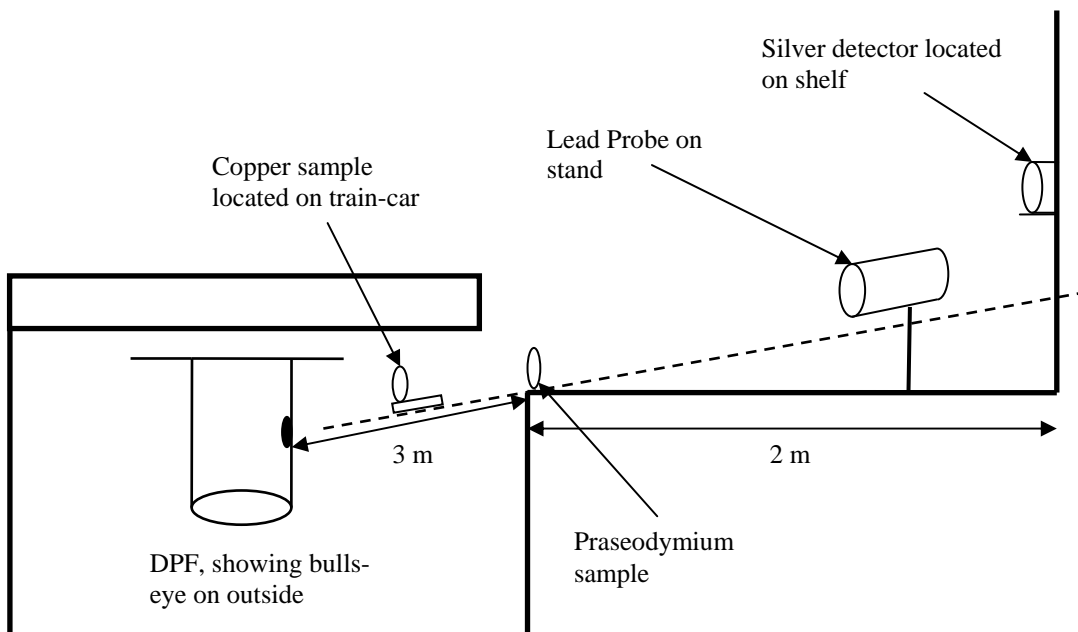
Figure 4: 2-D schematic diagram of building containing DPF and detector locations relative to the DPF. All samples had a direct line of sight to the bulls-eye on the DPF.

This method was used because the DPF was mounted in a tritium-contaminated pit, and there were no other access points to place the samples for irradiation. Further complicating the irradiation of the sources was the cover over the DPF pit, such that there was only a small solid angle where the sources could be placed while maintaining a direct line of sight to the bulls-eye on the DPF (Figure 5).

Figure 5: View into DPF Pit. The samples were aligned with a direct line of sight to the bulls-eye, which marked the approximate location of the pinch in the source.

Also, because the building housing the DPF was a radiation area, we had to set the coincidence systems up in the trailers used for controlling the DPF and have the sample activity measured by health physics prior to removal.

The D-T experiments were done by using a dense plasma focus provided by NSTec as a 14.1 MeV neutron source. The DPF used was a Mather-type pinch with maximum neutron yield of greater than 10^{12} neutrons per shot. The DPF operated using 133 kJ of stored energy with a

peak plasma current of 1.5 MA. For storing this energy prior to discharge, it was based off of 9 – 27 µF capacitors charged with a Marx generator with potential 35 kV.   The neutrons produced by D-T fusion reacted with the copper samples, which were then removed from the chamber and inserted into the counting system. To allow for the extrapolation of the number of atoms of the radioisotopes formed back to the initial time, the MCS software was triggered externally when the DPF fired.

For the individual shots, the copper samples that were used had dimensions of 1 cm diameter with 1 cm thickness, 1 inch (2.54 cm) diameter with ⅜ inch (.9525 cm) thickness, or 3 inch (7.62 cm) diameter with ⅜ inch (.9525 cm) thickness. For these samples, the counting efficiencies of the detectors were modeled based on the geometry in MCNP. The modeling was done by Dr. Gary Cooper, using a method that combined the factors for the detector efficiency, ε_D, and self absorption, ε_S, into a single factor. In doing this, it was determined that in the 6" diameter coincidence system for the 1 cm sample, the counting efficiency was 12.0%, for the 1 inch sample, the counting efficiency was 10.12%, and for the 3 inch sample the counting efficiency was 8.01%. For calibration using the 3" NaI coincidence system, the counting efficiency for the 3 inch sample was calculated to be 3.45%. Using these values, the *F* factor was calculated for the different samples and used to calculate the neutron yield of the given shot using Eq. 8.

Data:

Using the DPF from NSTec, a total of 11 D-T shots were taken with data counted on either the 6" NSTec coincidence system or the 3" NaI coincidence system, with one additional shot having data taken only on the 6" NIF coincidence system. For the data taken using the

different multi-channel scalers, I was tasked with the data analysis for the measurement of the

yield using the *F* factor method for the copper samples. Along with measurement of the yield, I

made a comparison of the yield measurements for the different coincidence systems and sample

sizes. The data from the praseodymium and silver was taken and analyzed by Tim Meehan and

Chris Hagan of NSTec, with the measurements using the lead probe analyzed by Alan Nelson of

Sandia National Labs.   For these experiments, either two or three copper samples were

irradiated on each firing of the DPF source. These samples were either counted solely in one of

the detectors or counted sequentially in two of the detectors to get a cross calibration between

detectors and different sample sizes. For analysis, it was most effective to plot the data for both

samples after subtracting an estimate of the background counts caused by natural background

radiation or the long-lived isotope, Cu-64. Subtracting the long-lived isotope is appropriate for

this calculation because the ratio of counts between the two radioisotopes formed by neutron

activation is small. It is also important because the activation in the Cu-64 cannot be directly

calculated, due the production of Cu-64 by neutron capture in the Cu-63. The threshold for

neutron capture is very low, such that a measurement of the yield from Cu-64 would be

artificially high as the production from the neutron capture is difficult to calculate. The ratio of

activation between the isotopes can be approximated by applying Eq. 1 to both samples, getting:

$$A_{62} = \lambda_{62}N_{62}, \quad A_{64} = \lambda_{64}N_{64}$$

$$\frac{A_{64}}{A_{62}} = \frac{\lambda_{64}N_{64}}{\lambda_{62}N_{62}} \approx \frac{\lambda_{64}\phi_n\sigma_{65}\varepsilon_{B65}N_{65}}{\lambda_{62}\phi_n\sigma_{63}\varepsilon_{B63}N_{63}} = \frac{\lambda_{64}\sigma_{65}\varepsilon_{A65}\varepsilon_{B65}}{\lambda_{62}\sigma_{63}\varepsilon_{A63}\varepsilon_{B63}}$$

$$\therefore \frac{A_{64}}{A_{62}} \approx \frac{.00091 \times 910 \times .3085 \times .19}{.0712 \times 450 \times .6915 \times .98} = .0022$$

Subtracting the approximated activation of the Cu-64 from the total activation, the activation for

the Cu-62 can be approximated, which is then used in producing a decay curve from the counting

data. An example of this is given for data recorded on the 6" NSTec system for the second shot, shown in Figures 6 and 7. For these plots, the background was dominated by the decay of the long-lived isotope, such that for Figure 6, the background is approximately 16 counts per minute, and for Figure 7, the background is approximately 750 counts per minute.

The equation shown on the plot:

$$y = 5{,}596\, e^{-0.0708x}$$
$$R^2 = 0.9892$$
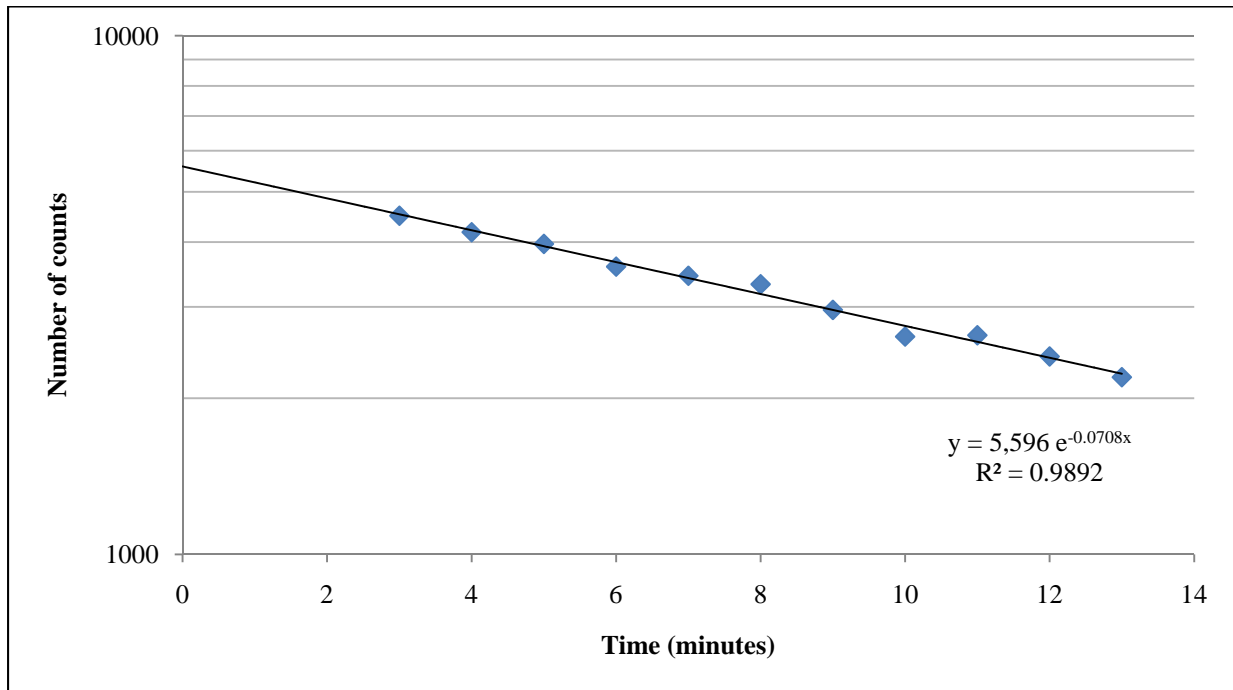
Figure 6: Plot of measured exponential decay and number of counts for 1 cm diameter, 1 cm thick sample, for second D-T DPF shot using 6" NSTec coincidence system from shot time through removal from coincidence unit
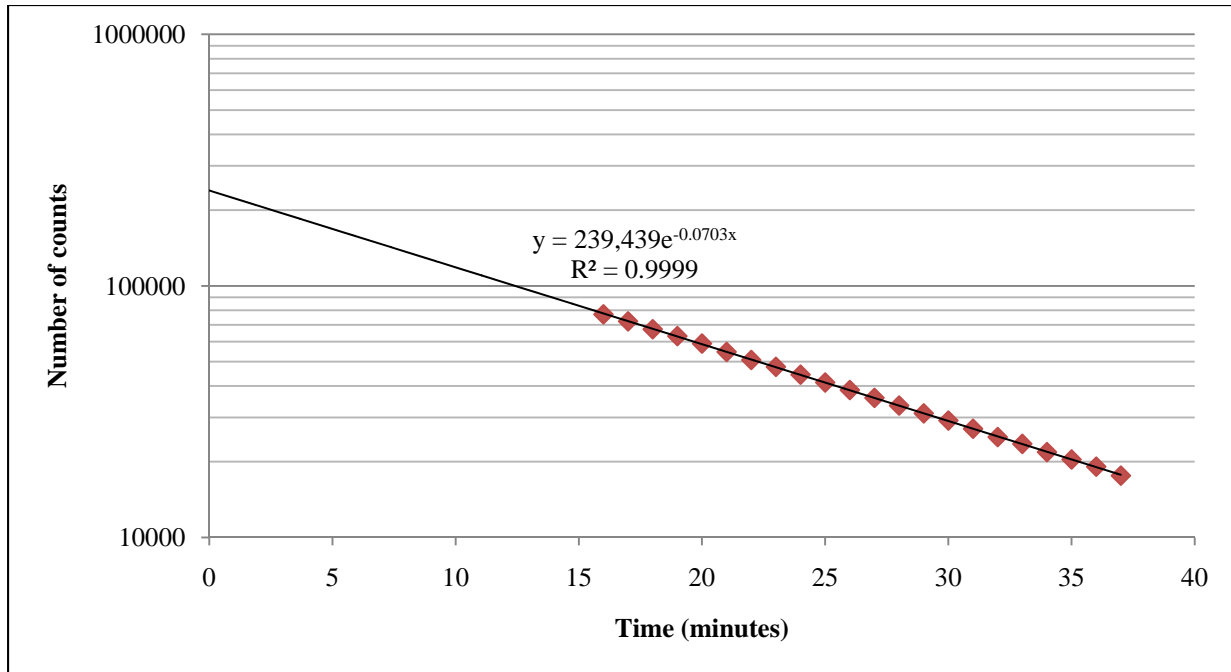
Figure 7: Plot of measured exponential decay and number of counts for 3 inch diameter, 3/8 inch (.9575 cm) sample for second D-T DPF shot using 6" NSTec coincidence system from shot time through removal from coincidence unit

In these plots, the number of counts recorded on the MCS is plotted on a semi-log scale with the

exponential fit of the data demonstrating a strong linear relationship in both cases. As this is the

case, the linearity of the plots satisfies the radioactive decay law, thereby validating the

functionality of the detectors by the demonstration of the expected result.

Results:

As the objective of this experiment was to cross-calibrate the copper activation systems

relative to each other, the different sample sizes, and the lead probe, silver detector and

praseodymium sample, the metric that is desired for observing this relationship is the total

neutron yield. To calculate the neutron yield, I used the F factor method, calculating the factor

for the different sample size and detector combinations as described earlier. I also used a

measured F factor for the 1 cm samples that was determined by a previous experiment by G. W.

Cooper, C. L. Ruiz, *et. al.*[19]. This was done to compare the yield using that factor to the F

factor calculated for these samples. The yield calculations given in Table 2 are those using the *F*

factor calculated for the specific samples and counting geometry. In doing this, the measured

yields for all the individual shots and detectors are given in Table 2, with the measured yield for

detectors with two different-sized samples counted being given as the average of the measured

yield from each sample. The large gaps in the table are due to shots where samples were not

counted in the detectors, there were errors in the MCS software and data was lost, or where the

previous sample was being counted for an extended period of time to allow for an observation of

the Cu-64 present.

Shot	Copper NIF system	Copper NSTec System	Copper 3" NaI System	Lead Probe	Praseodymium	Silver
1	$1.38 \pm .19$		$1.02 \pm .14$	1.46	1.53	1.42
2	$0.89 \pm .12$	$1.17 \pm .16$		1.19	1.34	1.26
3	$0.78 \pm .11$	$1.12 \pm .16$	$1.24 \pm .17$		2.28	1.86
4	$0.781 \pm .098$	$0.817 \pm .098$	$0.561 \pm .057$	1.02	1.11	1.05
5	$0.581 \pm .070$	$0.660 \pm .073$	$0.508 \pm .051$	0.904	1.00	0.970
6	$0.574 \pm .070$			0.919	1.03	0.980
7					0.479	0.450
8	$0.372 \pm .055$	$0.777 \pm .081$		0.540	0.645	0.600
9	$0.822 \pm .091$			1.16	1.36	1.20
10	$0.521 \pm .063$	$0.460 \pm .064$		0.712	0.844	0.780
11	$0.596 \pm .072$		$0.470 \pm .052$	0.723	0.884	1.20
12				0.203	0.275	0.230

Table 2: Calculated yields for all shots using dense plasma focus supplied by NSTec for data taken with copper samples counted in the NIF 6" NaI coincidence system, the NSTec 6" NaI coincidence system, or the 3" NaI coincidence system, along with yields calculated from lead probe, silver detector, and praseodymium sample. All values are given as (neutron yield) $\times\ 10^{-12}$. For shots where multiple copper samples were counted in the detectors, the yield is given as the average of the yield from each sample. Data for specific sample sizes is given in Appendix A.

To determine the quoted errors for the data samples, the errors from equipment malfunctions,

calculation of the *F* factor and counting statistics were propagated through to the final solution to

determine the overall error in the value. For the copper yields, the bulk of the error comes from

the calibration of the *F* factor method[19], with the exception of shots 1-3. Sometime when these

shots occurred, the tape slipped, so there was a 5 % uncertainty in the distance from the DPF

source to the samples.

Analysis:

From the plots of the radioactive decay of Cu-62 in the detectors, such as those in Figures 6 and 7, we can determine that the decay product was indeed Cu-62 and not dominated by another isotope or a false reading. This is the case because the 9.74 minute half-life of Cu-62 is significantly shorter than that of Cu-64 and approximately twice that of Cu-66. Also, because Cu-66 is not a positron emitter, the probability of it registering in the coincidence system is extremely low. This is due to the calibration of the time windows for the coincidence system to be on the order of 100 ns and the energy of the Cu-66 gamma ray being outside the SCA window for the 511 keV photon. The potential of these decay values being a false reading from the Ge-68 calibration source is small. If a portion of the Ge-68 source ended up being left in the system, either by fragmentation of the source or operator error, the half-life is 271 days, which would result in a significantly different decay curve than that of the Cu-62. Also, with this long half-life, the activity of the Ge-68 would change negligibly over the counting interval for the copper sample. Therefore, it would be appear to the detectors as a large source of background radiation, and would not noticeably affect the decay rate. As a result, we can look at the measured decay rate of the Cu-62 from the exponential fit for the data in Figures 6 and 7. For the two copper samples inserted in the detector, the measured decay constants were .0708 min^{-1} and .0703 min^{-1}, which correspond to half-lives of 9.79 minutes and 9.86 minutes, respectively. Comparing the half-lives of these samples to the accepted value for Cu-62, they are both within 1.5 % of the accepted value, thereby falling well within the margin of error for this experiment. Also, the R^2 values of .9892 and .9999 imply that the exponential fit is extremely accurate for modeling the data, so we can be certain that we were detecting the decay of Cu-62.
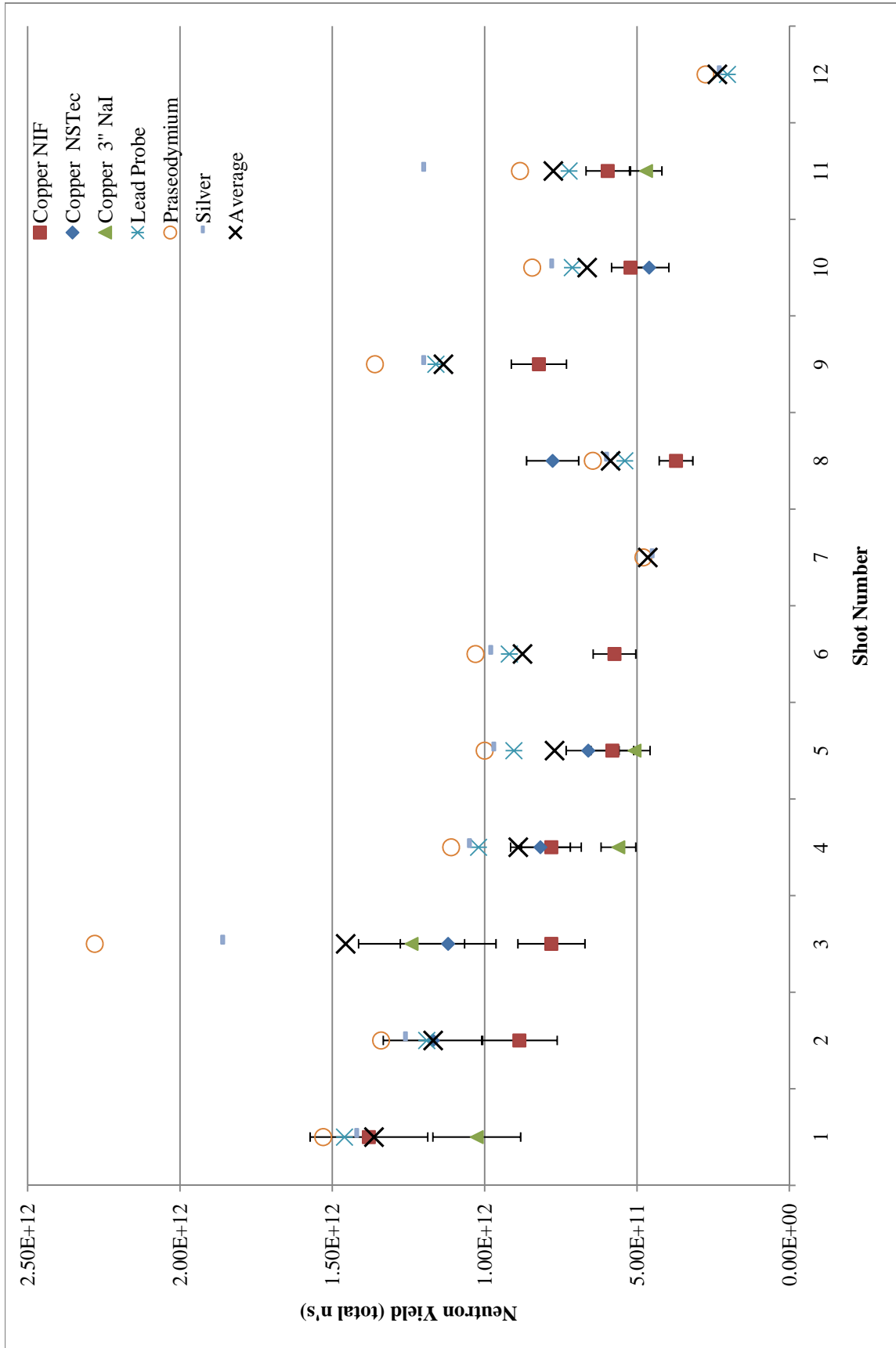
Figure 8: Plot of measured yield versus shot number for copper samples in 6" NIF coincidence system, 6" NSTec coincidence system, and 3" NaI coincidence system, using *F* factor method along with the yield measured using the lead probe, praseodymium sample and silver detector, and total average yield (Values also given in Table2)

The praseodymium sample consistently gave a higher reading than the other materials

used, with it being the largest calculated yield 75 % of the time. From this, it can be inferred that

the praseodymium likely gives an upper bound on the measured yield for the shot, and that there

is some effect in the counting system that results in the praseodymium producing more counts

than would be expected. To count the praseodymium, the sum-peak method was used instead of

the coincidence method as used for copper. This method allows in all the counting efficiencies

being cancelled out by other factors, however, the use of thin samples for the praseodymium

could result in positrons escaping the sample and annihilating in the NaI detector instead.   Even

if the measurement is high due to positrons escaping, the readings for the Pr-141 sample are still

generally within their 18% error as calculated by Meehan *et. al.*[21] As the lead probe is a

laboratory standard detector, and has been extensively calibrated, with the exception of the two

shots where there was an error and no data was recorded, it can be assumed that the lead value

would be the most consistent due to its fixed location and operating voltage. However, the low

threshold can allow for neutrons to scatter into the detector, and the calibration for a lead probe is

done at a distance of 12 – 18", such that the validity of the calibration at large distances is

uncertain. Another aspect with the lead is that its extremely short half-life for the lead-207

metastable state, coupled with its high detection efficiency and cross section, requires the

detector to be at a larger distance to prevent saturation in the plastic scintillator. For the copper

samples, the measured yields are generally closest to those of the silver samples, but usually

within the error margin of at least one of the other materials, be it the praseodymium or lead.

As one of the objectives for the experiment was to cross-calibrate the system relative to

different size samples, we looked at the measured yield for the samples individually. In doing

this, we were able to distinguish between the different sized samples and determine the relative

yields dependent on the sample sizes. It was especially beneficial to look at shots on the two 6"

NaI systems where there were two different sized samples irradiated and counted in the same

detector. This is the most beneficial data set because it allows for a determination of which

sample size is generally the most accurate relative to the lead, praseodymium, and silver. This in

turn helps determine which size samples will give the best results for experiments done at NIF.

The data for the different samples in the 6" NaI detectors on the different shots can be seen in

Figure 9.
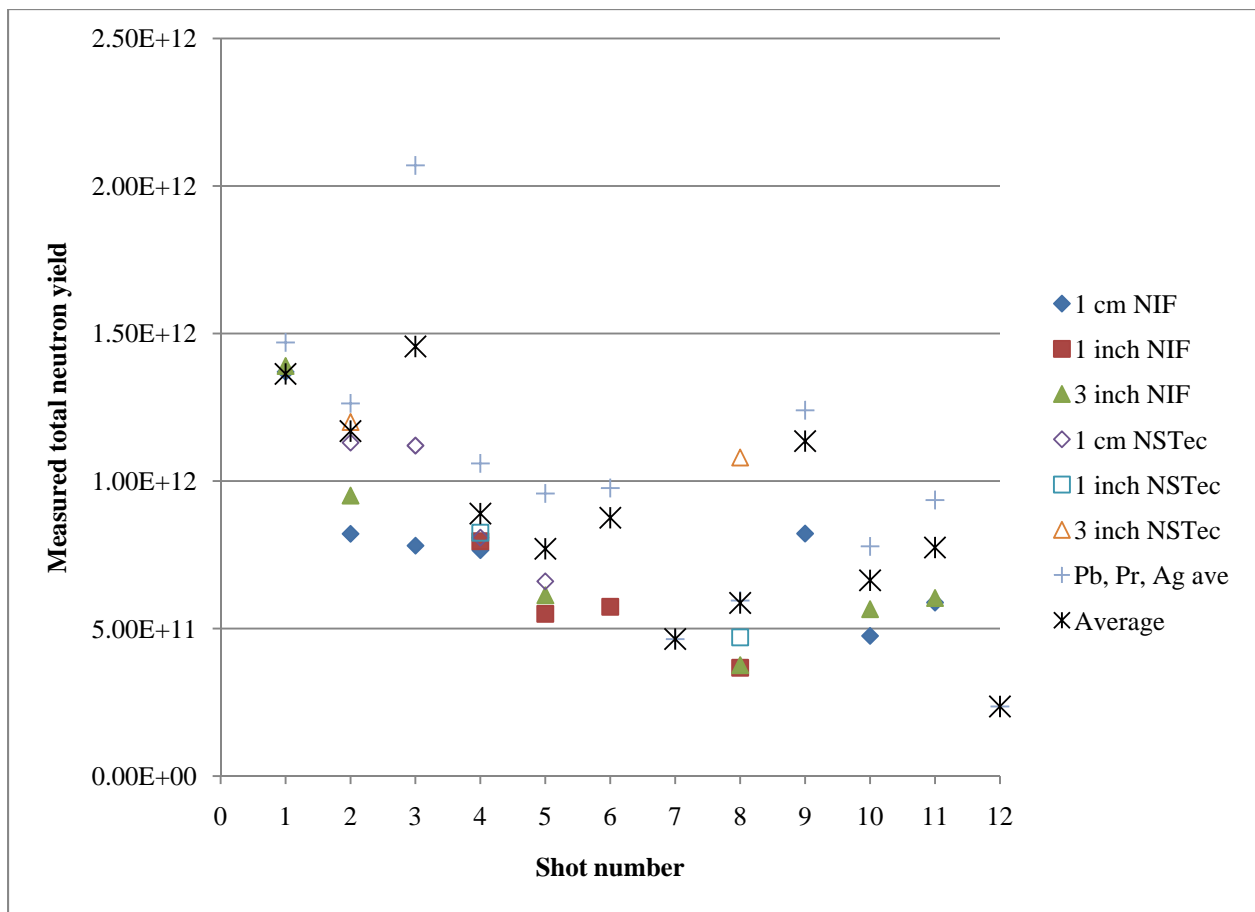
Figure 9: Measured total neutron yields for copper samples in 6" NaI coincidence systems discriminated by system and sample size and average measured yield from lead, praseodymium and silver activation along with overall average from all detectors

From Figure 9, it is evident that the 3 inch samples generally give the closest results for the

specific systems, as the only time where the 3" sample was further from the average value than

the smaller copper sample was for shot 8 in the NSTec system. This is reinforced further by the average ratio of measured yields between the copper samples and the lead, praseodymium and silver average, which can be seen in Table 3. From the data, it is even clearer that the 3 inch sample is the most accurate, as the average measured yields is 20% closer to the average yield for the lead, praseodymium and silver than the other samples. However, if we ignore the measured yield for the 3" sample counted in the NSTec system on shot 8, the ratio drops significantly, but ends up being 7.56×10^{-1}, which is still significantly closer than either of the other sample sizes.

Sample Size	1 cm × 1 cm	1 inch × ⅜ inch	3 inch × ⅜ inch
Ratio Y(Cu)/Y(Ave)	6.79×10^{-1}	6.83×10^{-1}	8.88×10^{-1}

Table 3: Average ratios of measured yield for specific sizes of copper samples in 6" NaI detectors to the average yield of the lead, praseodymium, and silver measurements

For the 1 cm × 1 cm samples, the calculated F factor is very close to the measured F factor from Cooper, *et. al*. As this is the case, the measured yield would be expected to also be close due to all other factors in the yield calculations being the same. From the ratio of the yields, it was determined that the yield measurement using the calculated F factor was approximately 2% less than the yield measurement using the previously determined F factor, such that $Y_{Calc}/Y_{Meas} = .98$. Because these yield measurements are both well within the error margin of the calculations (~10 %), there is no reason to believe that either the measured F factor from the earlier experiment or the calculated F factors are incorrect.

It is also evident that, in general, the measured yields for the copper samples are significantly lower than the measured yields calculated for the lead, praseodymium, and silver activation. This difference is evident for nearly all the samples counted in the 6" systems, and all of the shots counted in the 3" system. A possible explanation for this is the DPF wall, which is .375" thick and made of stainless steel. This wall was calculated into the F factor as a .25" thick

wall, such that the additional .125" would increase the amount of attenuation. As the *F* factors

for these data sets were calculated using the fundamental quantities for neutron reactions in the

material and the detector counting efficiencies, the presence of a thin wall that was not modeled

into the system would provide attenuation that would result in a low measurement of the total

neutron yield. However, since the unaccounted for portion of the wall is thin, the total

attenuation due to scattering in the wall would be small. This is because neutrons are one of the

most penetrating forms of ionizing radiation, and will generally pass through the material

without interacting enough for the scattering angle to be appreciable. In calculating the number

of neutrons that would scatter out of the sample, it was found that for a stainless steel DPF wall

of thickness .375" , the flux would decrease to 94.6 % of the value for a .25" thick wall. As

such, the measured yield would increase by 5.7 %, which results in a value closer to, but still less

than the other materials. However, this is possibly a reason for the lower yield measurement

using the *F* factor method, as it is unknown whether the yield measurements using the

praseodymium, lead, and silver correctly modeled the neutron attenuation due to the wall for

their calculations.   Also, because the trajectory of neutrons in air at STP is approximately linear,

there would be approximately no attenuation over the short distances between the DPF source

and the samples, and the decrease in counts due to scattering would be entirely due to the DPF

wall.

The second oddity in the calculated yields is the significant decrease in the yields for

those calculated using the *F* factor and the 3" NaI coincidence system. The calculated yield for

this system is not within the margin of error for any of the reference values (Pb, Pr, or Ag), and

only once within a margin of error for the yield measurements using the 6" NaI coincidence

systems. As this is the case, the most likely causes are the modeling and calculation of the

counting efficiency for the 3" detector, or some fault in the electronics. Because the calculations

for counting efficiencies were done using the assumption of 19.1 % efficiency for counting a

germanium-68 calibration source, the most likely reason that the values were consistently low is

that the counting efficiency of the 3" NaI system with a Ge-68 source is less than 19.1 %. If we

make this assumption, and further assume that the counting efficiencies modeled are half of what

they actually are, then all of the yield calculations would double and be within a margin of error

of at least one of the praseodymium, lead, and silver samples for all but the first shot. If we

assume that the actual counting efficiency is only 1.5 times the modeled value, then, with the

exception of shots 4 and 5, the calculated yield would fall in the middle of the Pr, Pb, and Ag

measurements. A final cause of this decrease could be the geometry detector system itself due to

the geometry dependence of the *F* factor calculation. Slight changes in the geometry due to a

dent in the casing or a detector becoming loose and moving slightly in the system could affect

the counting efficiency, but any such difference could change the measured yield by at most 1

percent, with a more reasonable estimate being $<.1$ %.

Looking at the exponential decay curves for the data series counted on the 3 inch NaI

coincidence system provided an interesting insight into the counting electronics used for the

experiment. For the samples counted in the 3" detector for both the first and third day of the

experiment, I noticed that the decay constant for these samples was noticeably less than the

accepted value, as is demonstrated in Figure 10. However, for the samples counted on the

second day of the experiment, the decay constants for the samples on the 3 inch system are

within 1 percent of the accepted value for copper-62.
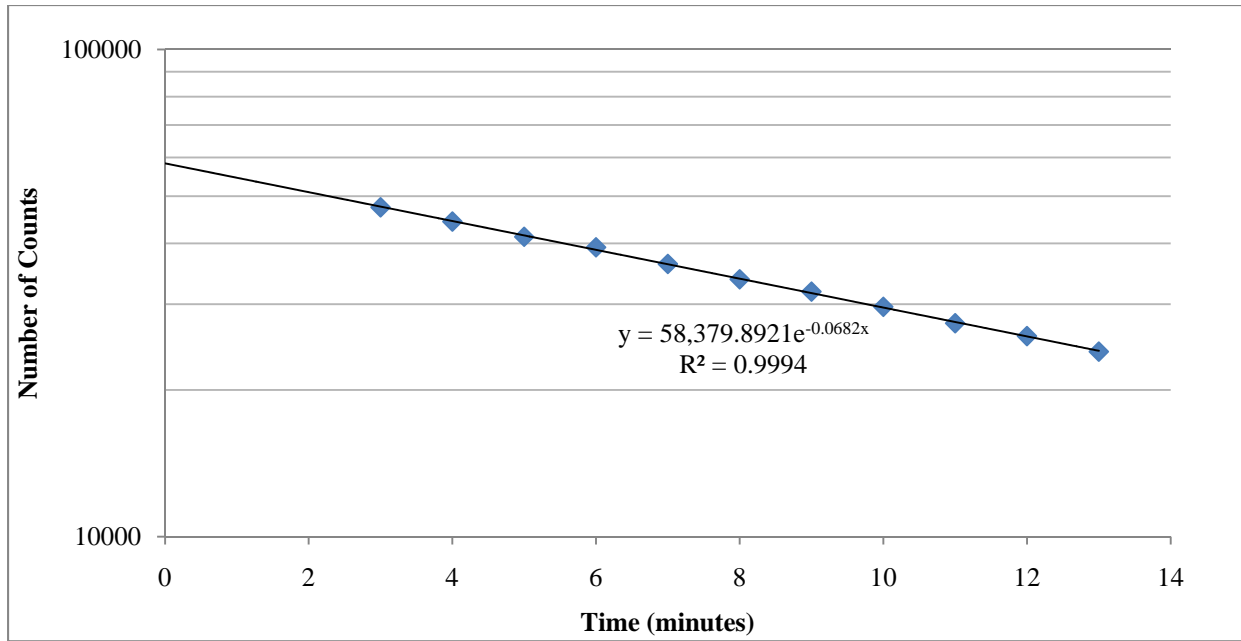
Figure 10: Exponential decay curve for 3 inch copper sample counted on 3" NaI coincidence system in Shot #4, demonstrating decay constant 4.2% less than accepted value

The fact that this occurred only for the 3 inch NaI system is interesting because the measurement

of the yield for these values was also consistently low. However, to calculate the yield, the

assumption was made that the half-life of copper-62 is known, and the yield was calculated using

an activity determined with that value for the decay constant. In doing this, the initial activity of

the sample that I used for the measurement of the yield is higher than the activity as determined

by propagating the exponential decay curve backwards in time. This means that the yield that I

calculated is greater than if calculated using the activity from the exponential fit of the decay.

Having discovered this discrepancy in the half-life, it was hypothesized that the cause of the

error is a malfunction in either the MCS board or the computer clock. The presence of an

intermittent problem in either the MCS or computer clock could result in the measured half-life

having large errors on some shots due to incorrect timing of the counting intervals by the

computer. These errors would change the measured half-life by associating a certain number of

counts with an incorrect interval. The cause of this problem is unknown, but may have been

related to the heat, as at least one of the computers overheated and shut down during the experiment. As these timing issues were first noticed recently, it would be beneficial to find the specific board and computer that were used with the 3" system to determine if there are problems with the internal clocks.

Sources of Error:

The significant sources of error for this experiment are systematic in nature dependent on the geometry for the irradiation of the samples. As the samples were being irradiated using a dense plasma focus which had a maximum output of $>10^{12}$ neutrons in a single pulse, it was necessary to have shielding in place and operate the DPF remotely to minimize the radiation exposure. This was important because the samples had to be lowered into the target chamber on a train car attached to a tape measure to determine their distance away from the source. This contributed to the sources of error because for shots 1-3, the tape slipped at some point, but was not noticed until the fourth shot, so the distance from the sample to the DPF source was estimated to be $(d_0 - 2.54) \pm 2.54$ cm. Although this amounts to an error of approximately 5 % in the distance from the source, as the shots were done at a distance of approximately 51 cm instead of 53.3 cm, the yield is dependent on the square of the distance. As such, the error in the calculated yield for the copper samples on these shots could be up to 10.25 %.

The second error that comes from the use of the dense plasma focus is that the geometry for the irradiation of the samples cannot be entirely determined as the angle of the samples relative to the DPF field pinch is only approximate. This affects the results because the neutron energies are not uniform over 4π, and has a desired angle of 95° relative to the orientation of the plasma current in the pinch for 14.1 MeV neutrons[19]. This angular dependence is due to the

conservation of momentum for ions in the plasma. At angles greater than 95°, the neutron energy is less than 14.1 MeV, whereas for angles less than 95°, the energy is greater than 14.1 MeV. Because the angle is partially unknown, but assumed to be close, the irradiation of the samples would differ slightly from the desired arrangement, which would result in the neutrons irradiating the samples having energy different than 14.1 MeV. This could have an effect on the measured yields by changing the cross sections for neutron interactions with the materials. However, none of the materials used have a spike or drop in the reaction cross section around 14 MeV, such that the difference in cross section should not be large enough to have a significant impact.

The second source of error was the thickness of the DPF wall, as its actual thickness was .125 inches thicker than its modeled thickness. Because the wall adds attenuation to the neutron beam, the measured yield was ~6 % less than if the attenuation was accounted for in the *F* factor. The greatest effect of this additional thickness is in the comparison between the copper samples and the other materials. If the attenuation was accounted for correctly by the researchers working with the other detectors, then the results from the copper are artificially low. As such, adjusting the yield corresponding to this additional attenuation will give a measured yield that is not only more accurate, but also more agreeable with the other data.

The third source of error is the design of the detectors and the use of the *F* factor for calculating the yield with different detectors. As the counting efficiencies were modeled for the 6" NaI coincidence system that is used for copper activation samples at the National Ignition Facility, and the data I worked with were for both 6" NaI systems, a possible difference in the coincidence system construction would have an effect on the yield. As both systems were constructed by the neutron activation group at Sandia Labs, the only difference between them

should be the NaI detectors as the NIF system uses newer detectors than the NSTec system. The effect of the different system on the yield calculation is unknown, as the exact interior dimensions and sizes of the NaI crystals could not be measured. The only known difference between the two is that the casings on the detectors in the NSTec system were iron, whereas the casings in the NIF system were aluminum due to a change in construction by the manufacturer. However, any differences should be small as both 6 inch coincidence systems were designed to be identical and the 3 inch system was designed to be similar to the Shiva copper activation system used by Lawrence Livermore National Laboratory for copper samples on NOVA[20].

Conclusions:

At National Security Technologies, we used a dense plasma focus containing a mixture of deuterium and tritium fuels to irradiate copper samples for a cross-calibration of 6" thallium-doped sodium-iodide and 3" NaI(Tl) detectors relative to a lead probe, silver detector and praseodymium samples. Using the (n,2n) reaction in copper to measure the 14.1 MeV neutrons produced by D-T fusion, we calibrated the *F* factor method for determining the neutron yield with these coincidence systems through the theoretical calculation of the *F* factor based off of fundamental quantities for the copper and the detector efficiency for the specific geometry. Having done so, we found that the measurement of the total neutron yield with the *F* factor method for copper activation is low compared to the measurement of the yield with lead, silver and praseodymium.

By comparing the neutron yield for the 6" coincidence system to that of the 3" system and the lead, praseodymium, and silver, we found that the measured yield for the 6" system is significantly closer to the other materials than the 3" system. As such we can conclude that as a

diagnostic for a large-scale experiment, such as the Laser Inertial Fusion Engine and National Ignition Campaign experiments at Lawrence Livermore National Laboratory, the 6" coincidence system will be the most effective for measuring the total neutron yield of the individual shots. Furthermore, by knowing the exact geometry and capsule irradiation for ICF experiments, the theoretical method of calculating the F factor will give an accurate measurement of the total neutron yield.

Finally, by comparing the ratios of the measured yields for different sizes of copper samples in the 6" NaI coincidence systems to the average yield from the lead, praseodymium, and silver, we found that the larger sample sizes resulted in ratios closer to one. For these samples, the most pronounced difference was going from the 1 inch sample to the 3 inch sample. The average measured yield for 3 inch samples was approximately 20 % closer to the average yield with the other materials than the average yield for the 1 inch. Also, we found that the yield calculated with the F factor method gives approximately the same answer for 1 cm diameter values as that using the measured F factor from G. W. Cooper, C. L. Ruiz *et. al.*[19]. As such, we concluded that for the copper activation detectors on NIF, of the samples tested at NSTec, it would be most beneficial to use the 3 inch diameter by ⅜ inch thick copper samples for measuring the total neutron yield. Furthermore, we concluded that for the 3 inch diameter samples, the measured total neutron yield would be 89 ± 10 % the average measured yield from praseodymium, lead, and silver samples.

<u>Proposed Further Research:</u>

To improve the experimental results, it would be beneficial to irradiate the samples in a more controlled geometry. This irradiation can be done using either a DPF for producing the D-

T neutrons, or with an ion beam, but should have the samples located at the desired angle relative to the source and at a more controlled length, rather than a variable length and uncertain angle. Doing this will allow for the measurement of a yield with more certainty due to the specific modeling of the system for this geometry, thereby giving a more accurate value for the theoretical *F* factor. Specifically, the ideal experiment would be to use an ion beam, such as the IBL at Sandia National Labs with a fixed target chamber. In doing this, the use of a velocity selector will result in a deuteron beam of nearly equal energy and associated particle counting in the beam will give a known beam current. Using these quantities, we can calculate an approximately absolute measurement of the number of neutrons that would be produced, allowing for a direct measurement of the *F* factor for any desired sample size, rather than having to calculate the factor for specific geometries and sample sizes. Furthermore, the use of an ion beam would allow for both pulsed neutrons and a steady-state 14.1 MeV neutron flux, which would allow for an exact calculation of the detector efficiency for copper samples.

The second experiment that would be beneficial is to measure the detector efficiency with sources of known activity. To do this, the two methods that would be most efficient would be to insert a germanium-68 source into the coincidence system or to saturate a copper sample to insert into the system. For the germanium source, the objective would be to count the 511 keV photons that occur from the decay of gallium-68 and determine the number that were detected in the system. For a copper sample, the use of a nuclear reactor or steady-state fission source (such as californium-252) will be able to saturate the sample to a known activity to count the 511 keV photons from the decay of Cu-62 and Cu-64. These methods are effective for determining the total detector efficiency because they allow for an absolute calculation of the activity of the sample. Then by simply taking the ratio of the measured activity against the decay of the

saturation activity, the coincidence system efficiency can be determined for measuring the beta decay in the samples.

References:

[1] S. Haan, Science and Technology Review. July/August 2010. Lawrence Livermore National Laboratory. pp. 4-11.

[2] P. Bode, *et. al.*, *Use of Research Reactors for Neutron Activation Analysis*, IAEA Advisory group meeting. IAEA-TECDOC-1215 (2001)

[3] D. De Soete, R. Gijbels, and J. Hoeste. *Neutron Activation Analysis*, Wiley Interscience, London. 1972.

[4] E. M. Baum, M. C. Ernesti, H. D. Knox, T. R. Miller, and A. M. Watson, *Nuclides and Isotopes: Chart of the Nuclides, 17th Edition*. Bechtel Marine Propulsion Corporation. 2010.

[5] F. L. Ribe, Rev. Mod. Phys., 47, 7, (1975).

[6] W.R. Arnold, *et. al.*, Physical Review, 93, 483 (1954)

[7] T. Kammash, *Fusion Reactor Physics, Principles and Technology*. Ann Arbor Science Publishers, 1975.

[8] C. L. Ruiz, R. J. Leeper, A. Schmidlapp, and G. W. Cooper, Rev. Sci. Instrum. 63, 4889 (1992)

[9]   C. Moreno, H. Bruzzone, J. Martínez, and A. Clausse, IEEE Trans. On Plasma Science 28, 1735 (2000)

[10] R. F. Post, Rev. Mod. Phys., 28, 338, (1956).

[11] J. O. Pouzo and M. M. Milanese, IEEE Trans. On Plasma Science 31, 1237 (2003)

[12] H. R. Lukens, Journal of Chemical Education, 44, 668 (1967)

[13] Nuclear Data Sheets 108 (2007) 1287.

[14] Brookhaven National Laboratory, Evaluated Nuclear Data File (ENDF) Retrieval & Plotting, http://www.nndc.bnl.gov/sigma/, (last accessed April 11, 2011).

[15] ASTM International, *Standard Test Method for Measuring Neutron Fluence and Average Energy from $^3H(d,n)^4He$ Neutron Generators by Radioactivation Techniques*. ASTM: E496 – 02

[16] V. Semkova, *et. al.,* Phys. Rev. C. 80, 024160, (2009)

[17] J.E. Turner, *Atoms, Radiation, and Radiation Protection, Third Edition*. Wiley-VCH, Weinheim: 2007.

[18] J. Spanier and E. M. Gelbard, *Monte Carlo Principles and Neutron Transport Problems*. Addison Wesley, Mineola, NY: 1997.

[19] G. W. Cooper and C. L. Ruiz, Rev. Sci. Instrum. 72, 814 (2001)

[20] R. A. Lereche, *Copper Activation System – Operator's Manual*. Interdepartmental memorandum DDG 79-108, Lawrence Livermore Laboratory, (1979)

[21] T. Meehan, E. C. Hagan, C.L. Ruiz, and G.W. Cooper, Nucl. Instrum. Methods Phys. Res. A 620. 397 (2010)

Shot	1 cm NIF	1 inch NIF	3 inch NIF	1 cm NSTec	1 inch NSTec	3 inch NSTec	Lead Probe	Praseodymium	Silver	Average
1	1.37E+12		1.39E+12				1.46E+12	1.53E+12	1.42E+12	1.36E+12
2	8.21E+11		9.51E+11	1.13E+12		1.20E+12	1.19E+12	1.34E+12	1.26E+12	1.17E+12
3	7.81E+11			1.12E+12				2.28E+12	1.86E+12	1.46E+12
4	7.66E+11	7.96E+11		8.08E+11	8.25E+11		1.02E+12	1.11E+12	1.05E+12	8.90E+11
5		5.50E+11	6.13E+11	6.60E+11			9.04E+11	1.00E+12	9.70E+11	7.71E+11
6		5.74E+11					9.19E+11	1.03E+12	9.80E+11	8.76E+11
7								4.79E+11	4.50E+11	4.65E+11
8		3.67E+11	3.76E+11		4.70E+11	1.08E+12	5.40E+11	6.45E+11	6.00E+11	5.87E+11
9	8.22E+11						1.16E+12	1.36E+12	1.20E+12	1.14E+12
10	4.75E+11		5.66E+11				7.12E+11	8.44E+11	7.80E+11	6.63E+11
11	5.88E+11		6.04E+11				7.23E+11	8.84E+11	1.20E+12	7.75E+11
12							2.03E+11	2.75E+11	2.30E+11	2.36E+11

In this table are all the values given for Figure 9 with the sample sizes for each of the copper samples used noted along with the detector the measurement came from. It should be noted that there are no error bars on the individual samples because these values are for a primarily qualitative observation of the yield relative to the samples. Only the 6" systems are shown because that size system is what is being used at the National Ignition Facility.

Appendix B – Raw Data:

Shot 1 – NIF System:

Samples Counted	Sample Mass (g)	Distance to DPF (cm)	Counting Order
1cm#7	6.34	50.8 ± 2.5	1
3inch#10	383.9	50.8 ± 2.5	2

Time (s)	Counts	Time(s)	Counts	Time(s)	Counts
0	13	2220	18617		
60	2	2280	17404		
120	4				
180	3924				
240	4815				
300	4544				
360	4210				
420	3737				
480	3670				
540	3435				
600	3127				
660	3014				
720	2770				
780	2496				
840	2431				
900	125				
960	5				
1020	78299				
1080	75260				
1140	70097				
1200	64764				
1260	59885				
1320	55312				
1380	51807				
1440	47527				
1500	44591				
1560	40782				
1620	38194				
1680	35059				
1740	32485				
1800	30745				
1860	28742				
1920	25937				
2040	22673				
2100	21408				
2160	19854				

Shot 1 – 3" NaI System:

Samples Counted	Sample Mass (g)	Distance to DPF (cm)	Counting Order
3inch#10	383.9	50.8 ± 2.5	1
1cm#7	6.34	50.8 ± 2.5	2

Time (s)	Counts	Time(s)	Counts	Time(s)	Counts
0	3	2220	284	4440	763
60	1	2280	270	4500	690
120	5759	2340	237	4560	657
180	65434	2400	212	4620	638
240	61586	2460	294	4680	617
300	57566	2520	4789	4740	609
360	54279	2580	4448	4800	560
420	50351	2640	4213	4860	592
480	47147	2700	3899	4920	493
540	44116	2760	3726	4980	527
600	41424	2820	3467	5040	477
660	39428	2880	3184	5100	467
720	36891	2940	2959	5160	444
780	34146	3000	2780	5220	453
840	31785	3060	2676	5280	432
900	27431	3120	2540	5340	430
960	580	3180	2285	5400	449
1020	1131	3240	2231	5460	433
1080	1050	3300	2025	5520	389
1140	989	3360	1934	5580	401
1200	914	3420	1770	5640	403
1260	912	3480	1684	5700	402
1320	821	3540	1644	5760	356
1380	748	3600	1544	5820	400
1440	710	3660	1415		
1500	713	3720	1397		
1560	637	3780	1295		
1620	541	3840	1214		
1680	526	3900	1139		
1740	514	3960	1077		
1800	448	4020	1068		
1860	456	4080	910		
1920	402	4140	935		
1980	393	4200	884		
2040	355	4260	847		
2100	313	4320	837		
2160	308	4380	772		

Shot 2 – NIF System:

Samples Counted	Sample Mass (g)	Distance to DPF (cm)	Counting Order
3inch#15	384.52	50.8 ± 2.5	1
1cm#13	6.28	50.8 ± 2.5	2

Time (s)	Counts	Time(s)	Counts	Time(s)	Counts
0	6	2220	307		
60	2				
120	7778				
180	158372				
240	144950				
300	131088				
360	119954				
420	108731				
480	99232				
540	90429				
600	82646				
660	76420				
720	70368				
780	65301				
840	4626				
900	1362				
960	1218				
1020	1097				
1080	1054				
1140	1023				
1200	901				
1260	858				
1320	826				
1380	784				
1440	731				
1500	611				
1560	593				
1620	536				
1680	500				
1740	489				
1800	464				
1860	427				
1920	412				
1980	429				
2040	356				
2100	308				
2160	337				

Shot 2 – NSTec System:

Samples Counted	Sample Mass (g)	Distance to DPF (cm)	Counting Order
1cm#13	6.28	50.8 ± 2.5	1
3inch#15	384.52	50.8 ± 2.5	2

Time (s)	Counts	Time(s)	Counts	Time(s)	Counts
0	10	2220	18355		
60	1				
120	504				
180	4514				
240	4197				
300	3985				
360	3603				
420	3460				
480	3334				
540	2976				
600	2645				
660	2661				
720	2423				
780	2211				
840	166				
900	18550				
960	77851				
1020	73059				
1080	68035				
1140	63909				
1200	59755				
1260	55418				
1320	51504				
1380	48417				
1440	45141				
1500	42078				
1560	39306				
1620	36650				
1680	34199				
1740	31903				
1800	29915				
1860	27804				
1920	25812				
1980	24304				
2040	22602				
2100	21158				
2160	19867				

Shot 3 – NIF System:

Samples Counted	Sample Mass (g)	Distance to DPF (cm)
1cm#5	5.96	47.2 ± 2.5

Time (s)	Counts	Time(s)	Counts	Time(s)	Counts
0	3	2340	277	4680	38
60	3	2400	251	4740	34
120	2037	2460	277	4800	36
180	3087	2520	210	4860	26
240	2926	2580	202	4920	27
300	2805	2640	202	4980	29
360	2581	2700	198	5040	27
420	2445	2760	188	5100	32
480	2293	2820	140	5160	23
540	2139	2880	178	5220	29
600	1941	2940	157	5280	23
660	1915	3000	126	5340	31
720	1786	3060	106	5400	19
780	1580	3120	110	5460	37
840	1493	3180	128	5520	21
900	1374	3240	107	5580	32
960	1289	3300	108	5640	30
1020	1267	3360	102	5700	21
1080	1173	3420	79	5760	18
1140	1077	3480	70	5820	14
1200	992	3540	75	5880	20
1260	1025	3600	72	5940	26
1320	812	3660	79	6000	23
1380	811	3720	65	6060	22
1440	778	3780	61	6120	18
1500	761	3840	66	6180	17
1560	642	3900	71	6240	26
1620	614	3960	64	6300	23
1680	598	4020	47	6360	17
1740	501	4080	53	6420	16
1800	540	4140	35	6480	23
1860	470	4200	36	6540	17
1920	478	4260	37	6600	16
1980	443	4320	33	6660	18
2040	413	4380	47	6720	21
2100	383	4440	44	6780	28
2160	338	4500	39	6840	16
2220	326	4560	42	6900	20
2280	294	4620	42	6960	24

Time (s)	Counts	Time(s)	Counts	Time(s)	Counts
7020	22	9660	20	12360	23
7080	23	9720	16	12420	13
7140	21	9780	13	12480	18
7200	19	9840	22	12540	25
7260	17	9900	19	12600	15
7320	16	9960	13	12660	19
7380	24	10020	19	12720	19
7440	14	10080	12	12780	14
7500	19	10140	11	12840	10
7560	14	10200	16	12900	24
7620	12	10260	25	12960	15
7680	12	10320	13	13020	25
7740	16	10380	14	13080	15
7800	18	10440	18	13140	15
7860	18	10500	17	13200	14
7920	21	10560	16	13260	17
7980	13	10620	17	13320	18
8040	19	10680	16	13380	19
8100	10	10740	19	13440	23
8160	16	10800	24	13500	22
8220	16	10860	15	13560	13
8280	27	10920	15	13620	19
8340	21	10980	14	13680	11
8400	12	11040	25	13740	20
8460	15	11100	11	13800	20
8520	23	11160	19	13860	15
8580	25	11220	14	13920	12
8640	21	11280	17	13980	10
8700	24	11340	18	14040	23
8760	17	11400	30	14100	25
8820	19	11460	14	14160	14
8880	19	11520	21	14220	13
8940	16	11580	13	14280	21
9000	30	11640	14	14340	19
9060	16	11700	15	14400	12
9120	10	11760	33	14460	22
9180	19	11820	10	14520	15
9240	17	11880	13	14580	10
9300	17	11940	16	14640	16
9360	14	12000	24	14700	18
9420	12	12060	26	14760	16
9480	8	12120	17	14820	13
9540	15	12180	14	14880	14
9600	12	12240	22	14940	17

Time (s)	Counts	Time(s)	Counts	Time(s)	Counts
15000	26	17640	11	20280	20
15060	19	17700	18	20340	8
15120	21	17760	13	20400	19
15180	18	17820	16	20460	12
15240	23	17880	15	20520	11
15300	16	17940	12	20580	22
15360	14	18000	16	20640	14
15420	16	18060	15	20700	17
15480	15	18120	15	20760	12
15540	11	18180	16	20820	18
15600	17	18240	24	20880	12
15660	17	18300	22	20940	20
15720	20	18360	11	21000	10
15780	15	18420	17	21060	17
15840	15	18480	16	21120	17
15900	21	18540	7	21180	19
15960	17	18600	14	21240	18
16020	13	18660	14	21300	18
16080	18	18720	17	21360	16
16140	17	18780	14	21420	19
16200	19	18840	20	21480	15
16260	16	18900	19	21540	12
16320	22	18960	16	21600	18
16380	18	19020	18	21660	20
16440	15	19080	16	21720	13
16500	15	19140	18	21780	12
16560	18	19200	14	21840	18
16620	17	19260	18	21900	16
16680	24	19320	17	21960	10
16740	21	19380	17	22020	17
16800	11	19440	12	22080	25
16860	16	19500	12	22140	10
16920	15	19560	17	22200	12
16980	27	19620	10	22260	12
17040	16	19680	9	22320	21
17100	19	19740	17	22380	15
17160	9	19800	17	22440	15
17220	18	19860	13	22500	13
17280	13	19920	24	22560	15
17340	10	19980	12	22620	21
17400	10	20040	18	22680	18
17460	13	20100	21	22740	19
17520	23	20160	22	22800	16
17580	11	20220	13	22860	19

Shot 3 – NSTec System:

Samples Counted	Sample Mass (g)	Distance to DPF (cm)
1cm#10	6.3	47.2 ± 2.5

Time (s)	Counts	Time(s)	Counts	Time(s)	Counts
0	5	2340	353	4680	34
60	5	2400	325	4740	39
120	3492	2460	341	4800	37
180	4509	2520	281	4860	31
240	4145	2580	282	4920	33
300	3921	2640	277	4980	36
360	3569	2700	229	5040	34
420	3416	2760	198	5100	34
480	3134	2820	192	5160	43
540	2898	2880	208	5220	34
600	2740	2940	178	5280	40
660	2497	3000	211	5340	18
720	2323	3060	163	5400	18
780	2129	3120	136	5460	38
840	2055	3180	140	5520	25
900	1888	3240	136	5580	29
960	1746	3300	129	5640	33
1020	1677	3360	123	5700	37
1080	1637	3420	96	5760	29
1140	1452	3480	100	5820	25
1200	1305	3540	93	5880	22
1260	1248	3600	104	5940	31
1320	1172	3660	91	6000	27
1380	1055	3720	87	6060	16
1440	1050	3780	91	6120	13
1500	951	3840	64	6180	32
1560	863	3900	84	6240	26
1620	874	3960	68	6300	22
1680	791	4020	66	6360	24
1740	752	4080	72	6420	23
1800	637	4140	60	6480	23
1860	655	4200	64	6540	21
1920	578	4260	65	6600	20
1980	526	4320	59	6660	17
2040	526	4380	43	6720	28
2100	465	4440	40	6780	16
2160	451	4500	44	6840	21
2220	434	4560	39	6900	24
2280	397	4620	44	6960	27

Time (s)	Counts	Time(s)	Counts	Time(s)	Counts
7020	17	9660	20	12360	22
7080	27	9720	16	12420	19
7140	19	9780	27	12480	19
7200	21	9840	18	12540	16
7260	18	9900	21	12600	19
7320	25	9960	24	12660	13
7380	13	10020	13	12720	29
7440	19	10080	14	12780	15
7500	24	10140	31	12840	9
7560	18	10200	18	12900	18
7620	25	10260	21	12960	28
7680	16	10320	13	13020	21
7740	21	10380	25	13080	20
7800	28	10440	18	13140	14
7860	16	10500	18	13200	21
7920	18	10560	18	13260	13
7980	15	10620	19	13320	14
8040	16	10680	12	13380	20
8100	24	10740	22	13440	16
8160	26	10800	15	13500	17
8220	19	10860	16	13560	16
8280	18	10920	22	13620	19
8340	15	10980	20	13680	23
8400	23	11040	16	13740	18
8460	19	11100	18	13800	26
8520	18	11160	26	13860	19
8580	25	11220	19	13920	19
8640	10	11280	22	13980	22
8700	27	11340	18	14040	14
8760	22	11400	18	14100	14
8820	21	11460	17	14160	23
8880	17	11520	17	14220	18
8940	21	11580	17	14280	20
9000	17	11640	10	14340	13
9060	15	11700	15	14400	19
9120	18	11760	18	14460	15
9180	24	11820	12	14520	19
9240	20	11880	14	14580	18
9300	17	11940	21	14640	21
9360	19	12000	13	14700	19
9420	18	12060	17	14760	9
9480	13	12120	29	14820	17
9540	14	12180	19	14880	17
9600	20	12240	16	14940	20

Time (s)	Counts	Time(s)	Counts	Time(s)	Counts
15000	24	17640	18	20280	15
15060	17	17700	18	20340	14
15120	19	17760	19	20400	15
15180	19	17820	14	20460	10
15240	16	17880	23	20520	22
15300	14	17940	26	20580	14
15360	15	18000	19	20640	19
15420	17	18060	20	20700	16
15480	17	18120	12	20760	17
15540	23	18180	17	20820	14
15600	17	18240	17	20880	10
15660	15	18300	19	20940	13
15720	13	18360	13	21000	16
15780	14	18420	13	21060	17
15840	16	18480	14	21120	13
15900	18	18540	9	21180	17
15960	14	18600	19	21240	14
16020	12	18660	17	21300	19
16080	22	18720	17	21360	23
16140	18	18780	15	21420	13
16200	14	18840	14	21480	19
16260	13	18900	16	21540	15
16320	19	18960	13	21600	14
16380	24	19020	20	21660	14
16440	16	19080	17	21720	14
16500	20	19140	12	21780	15
16560	25	19200	13	21840	20
16620	13	19260	20	21900	24
16680	10	19320	22	21960	22
16740	11	19380	14	22020	18
16800	22	19440	19	22080	11
16860	16	19500	13	22140	21
16920	15	19560	13	22200	15
16980	15	19620	19	22260	22
17040	15	19680	17	22320	12
17100	20	19740	22	22380	15
17160	14	19800	18	22440	13
17220	15	19860	10	22500	11
17280	18	19920	15	22560	21
17340	21	19980	10	22620	15
17400	19	20040	12	22680	26
17460	19	20100	19	22740	11
17520	21	20160	14	22800	21
17580	14	20220	25	22860	16

Shot 3 – 3" NaI System:

Samples Counted	Sample Mass (g)	Distance to DPF (cm)
1cm#3	6.24	47.2 ± 2.5

Time (s)	Counts	Time(s)	Counts	Time(s)	Counts
0	1	2340	204	4680	13
60	8	2400	218	4740	24
120	2338	2460	175	4800	15
180	2633	2520	185	4860	21
240	2463	2580	150	4920	16
300	2288	2640	157	4980	15
360	2181	2700	117	5040	15
420	2038	2760	133	5100	26
480	1877	2820	129	5160	16
540	1783	2880	114	5220	15
600	1596	2940	129	5280	18
660	1493	3000	107	5340	18
720	1457	3060	105	5400	16
780	1349	3120	104	5460	11
840	1220	3180	91	5520	8
900	1204	3240	83	5580	18
960	1096	3300	74	5640	14
1020	976	3360	102	5700	27
1080	928	3420	75	5760	10
1140	881	3480	65	5820	11
1200	849	3540	55	5880	7
1260	744	3600	73	5940	9
1320	736	3660	55	6000	15
1380	702	3720	57	6060	12
1440	615	3780	50	6120	14
1500	514	3840	44	6180	15
1560	498	3900	53	6240	11
1620	471	3960	32	6300	15
1680	451	4020	45	6360	18
1740	437	4080	24	6420	21
1800	393	4140	47	6480	13
1860	349	4200	36	6540	11
1920	324	4260	30	6600	20
1980	311	4320	49	6660	9
2040	294	4380	27	6720	13
2100	282	4440	33	6780	12
2160	275	4500	22	6840	15
2220	230	4560	24	6900	10
2280	239	4620	20	6960	11

Time (s)	Counts	Time(s)	Counts	Time(s)	Counts
7020	7	9660	9	12360	17
7080	7	9720	13	12420	9
7140	14	9780	14	12480	12
7200	8	9840	25	12540	12
7260	9	9900	5	12600	17
7320	13	9960	12	12660	18
7380	11	10020	12	12720	13
7440	10	10080	12	12780	7
7500	11	10140	20	12840	22
7560	17	10200	13	12900	9
7620	9	10260	16	12960	8
7680	12	10320	18	13020	13
7740	15	10380	12	13080	10
7800	19	10440	10	13140	8
7860	17	10500	21	13200	12
7920	14	10560	11	13260	19
7980	19	10620	11	13320	17
8040	9	10680	9	13380	7
8100	16	10740	14	13440	11
8160	13	10800	13	13500	13
8220	15	10860	16	13560	15
8280	9	10920	9	13620	18
8340	15	10980	18	13680	10
8400	13	11040	15	13740	8
8460	13	11100	14	13800	7
8520	10	11160	21	13860	11
8580	10	11220	10	13920	14
8640	11	11280	16	13980	17
8700	8	11340	17	14040	7
8760	15	11400	13	14100	17
8820	8	11460	8	14160	14
8880	18	11520	6	14220	10
8940	11	11580	11	14280	13
9000	9	11640	13	14340	14
9060	10	11700	11	14400	17
9120	16	11760	14	14460	18
9180	13	11820	11	14520	10
9240	19	11880	11	14580	12
9300	7	11940	11	14640	13
9360	10	12000	15	14700	15
9420	15	12060	10	14760	12
9480	8	12120	9	14820	8
9540	13	12180	20	14880	9
9600	17	12240	11	14940	6

Time (s)	Counts	Time(s)	Counts	Time(s)	Counts
15000	9	17640	11	20280	11
15060	10	17700	17	20340	12
15120	10	17760	9	20400	9
15180	14	17820	14	20460	9
15240	5	17880	10	20520	16
15300	8	17940	4	20580	12
15360	9	18000	10	20640	17
15420	17	18060	10	20700	6
15480	14	18120	10	20760	9
15540	5	18180	12	20820	8
15600	12	18240	12	20880	14
15660	11	18300	15	20940	13
15720	14	18360	5	21000	12
15780	10	18420	9	21060	14
15840	12	18480	3	21120	8
15900	9	18540	13	21180	9
15960	9	18600	9	21240	12
16020	14	18660	11	21300	12
16080	10	18720	5	21360	17
16140	14	18780	8	21420	17
16200	14	18840	10	21480	18
16260	7	18900	14	21540	3
16320	9	18960	16	21600	11
16380	12	19020	9	21660	12
16440	17	19080	9	21720	8
16500	14	19140	15	21780	7
16560	12	19200	12	21840	12
16620	11	19260	15	21900	12
16680	7	19320	10	21960	4
16740	6	19380	11	22020	15
16800	6	19440	12	22080	18
16860	11	19500	5	22140	12
16920	7	19560	14	22200	14
16980	10	19620	14	22260	8
17040	17	19680	9	22320	8
17100	14	19740	10	22380	16
17160	9	19800	8	22440	7
17220	12	19860	5	22500	15
17280	7	19920	12	22560	21
17340	14	19980	13	22620	16
17400	15	20040	10	22680	12
17460	11	20100	11	22740	8
17520	12	20160	10	22800	16
17580	9	20220	9	22860	6

Shot 4 – NIF System:

Samples Counted	Sample Mass (g)	Distance to DPF (cm)	Counting Order
1cm#1	6.32	44.29	1
1inch#19	41.56	44.29	2

Time (s)	Counts	Time(s)	Counts	Time(s)	Counts
0	4	2220	1957		
60	2	2280	1799		
120	2	2340	1631		
180	3600				
240	3413				
300	3245				
360	2965				
420	2736				
480	2635				
540	2324				
600	2277				
660	2040				
720	1905				
780	1783				
840	139				
900	6015				
960	8326				
1020	7789				
1080	7407				
1140	6850				
1200	6300				
1260	5933				
1320	5499				
1380	5106				
1440	4778				
1500	4502				
1560	4049				
1620	3861				
1680	3620				
1740	3371				
1800	3187				
1860	2963				
1920	2674				
1980	2482				
2040	2412				
2100	2190				
2160	2067				

Shot 4 – NSTec System:

Samples Counted	Sample Mass (g)	Distance to DPF (cm)	Counting Order
1inch#19	41.56	44.29	1
1cm#1	6.32	44.29	2

Time (s)	Counts	Time(s)	Counts	Time(s)	Counts
0	8	2220	369		
60	1	2280	331		
120	4965	2340	295		
180	21819				
240	20672				
300	19204				
360	17463				
420	16391				
480	15526				
540	14347				
600	13424				
660	12436				
720	11762				
780	10877				
840	3704				
900	1598				
960	1487				
1020	1474				
1080	1385				
1140	1182				
1200	1153				
1260	1078				
1320	984				
1380	977				
1440	870				
1500	820				
1560	740				
1620	708				
1680	661				
1740	655				
1800	535				
1860	520				
1920	501				
1980	470				
2040	469				
2100	397				
2160	378				

Shot 4 – 3" NaI System:

Samples Counted	Sample Mass (g)	Distance to DPF (cm)
3 inch #7	386.7	44.29

Time (s)	Counts	Time(s)	Counts	Time(s)	Counts
0	4				
60	4				
120	8902				
180	47631				
240	44543				
300	41452				
360	39451				
420	36484				
480	33950				
540	32028				
600	29833				
660	27615				
720	26003				
780	24168				
840	22675				
900	20964				
960	19545				
1020	18391				
1080	17206				
1140	16450				
1200	14774				
1260	14001				
1320	13166				
1380	12147				
1440	11487				
1500	10605				
1560	9876				
1620	9178				
1680	8445				
1740	8053				
1800	7480				
1860	7087				
1920	6608				
1980	6111				
2040	5735				
2100	5355				
2160	4906				
2220	4627				
2280	4361				

Shot 5 – NIF System:

Samples Counted	Sample Mass (g)	Distance to DPF (cm)	Counting Order
3 inch #17	384.86	44.29	1
1 inch #14	41.28	44.29	2

Time (s)	Counts	Time(s)	Counts	Time(s)	Counts
0	7	2220	1385	4440	169
60	2	2280	1262	4500	138
120	10755	2340	1230	4560	139
180	124019	2400	1128	4620	155
240	115240	2460	1043	4680	138
300	105893	2520	923		
360	97409	2580	915		
420	89433	2640	831		
480	82004	2700	818		
540	75715	2760	755		
600	69100	2820	683		
660	63707	2880	681		
720	58790	2940	641		
780	53976	3000	604		
840	3541	3060	547		
900	4692	3120	526		
960	5719	3180	501		
1020	5351	3240	450		
1080	5015	3300	420		
1140	4636	3360	395		
1200	4376	3420	371		
1260	4074	3480	407		
1320	3760	3540	312		
1380	3666	3600	322		
1440	3298	3660	305		
1500	3091	3720	280		
1560	2916	3780	279		
1620	2625	3840	276		
1680	2499	3900	255		
1740	2309	3960	239		
1800	2160	4020	230		
1860	1984	4080	194		
1920	1908	4140	176		
1980	1815	4200	228		
2040	1669	4260	171		
2100	1571	4320	189		
2160	1452	4380	167		

Shot 5 – NSTec System:

Samples Counted	Sample Mass (g)	Distance to DPF (cm)
1 cm #1	6.32	44.29

Time (s)	Counts	Time(s)	Counts	Time(s)	Counts
0	1	2340	253	4680	27
60	4	2400	223	4740	33
120	2	2460	203	4800	27
180	3046	2520	202	4860	32
240	2863	2580	184	4920	24
300	2695	2640	207	4980	25
360	2543	2700	157	5040	21
420	2239	2760	163	5100	29
480	2177	2820	158	5160	30
540	2094	2880	130	5220	25
600	1886	2940	118	5280	24
660	1778	3000	129	5340	26
720	1710	3060	115	5400	24
780	1570	3120	114	5460	18
840	1402	3180	100	5520	21
900	1425	3240	97	5580	18
960	1227	3300	77	5640	26
1020	1176	3360	86	5700	21
1080	1100	3420	81	5760	13
1140	985	3480	73	5820	24
1200	902	3540	70	5880	16
1260	943	3600	67	5940	25
1320	808	3660	70	6000	15
1380	833	3720	54	6060	21
1440	707	3780	46	6120	24
1500	611	3840	56	6180	12
1560	588	3900	52	6240	22
1620	577	3960	39	6300	14
1680	497	4020	50	6360	15
1740	523	4080	57	6420	14
1800	451	4140	50	6480	13
1860	416	4200	34	6540	14
1920	414	4260	28	6600	17
1980	347	4320	31	6660	17
2040	343	4380	31	6720	27
2100	322	4440	53	6780	14
2160	330	4500	22	6840	16
2220	303	4560	26	6900	8
2280	267	4620	24	6960	18

Time (s)	Counts	Time(s)	Counts	Time(s)	Counts
7020	11	9660	18		
7080	7	9720	18		
7140	17	9780	11		
7200	18				
7260	19				
7320	17				
7380	17				
7440	14				
7500	14				
7560	12				
7620	15				
7680	19				
7740	11				
7800	12				
7860	10				
7920	11				
7980	14				
8040	20				
8100	11				
8160	14				
8220	22				
8280	15				
8340	13				
8400	11				
8460	12				
8520	18				
8580	21				
8640	9				
8700	20				
8760	14				
8820	17				
8880	13				
8940	21				
9000	7				
9060	11				
9120	13				
9180	12				
9240	18				
9300	20				
9360	15				
9420	10				
9480	9				
9540	13				
9600	13				

Shot 5 – 3" NaI System:

Samples Counted	Sample Mass (g)	Distance to DPF (cm)	Counting Order
1 inch #14	41.28	44.29	1
3 inch #17	384.86	44.29	2

Time (s)	Counts	Time(s)	Counts	Time(s)	Counts
0	0	2220	3900	4440	424
60	0	2280	3611	4500	384
120	0	2340	3401	4560	407
180	4517	2400	3156	4620	374
240	8988	2460	2989	4680	387
300	8678	2520	2813	4740	372
360	7915	2580	2657	4800	335
420	7486	2640	2323	4860	359
480	7114	2700	2183	4920	326
540	6585	2760	2187	4980	310
600	5916	2820	1986	5040	323
660	5492	2880	1893	5100	296
720	5281	2940	1794	5160	276
780	4869	3000	1608	5220	273
840	1431	3060	1524	5280	266
900	18107	3120	1424	5340	267
960	16798	3180	1411	5400	220
1020	15375	3240	1290	5460	240
1080	14408	3300	1144	5520	235
1140	13638	3360	1074	5580	248
1200	12765	3420	1021	5640	240
1260	11867	3480	1009	5700	241
1320	10928	3540	930	5760	220
1380	10320	3600	909	5820	206
1440	9598	3660	854	5880	221
1500	9033	3720	842	5940	204
1560	8505	3780	773	6000	216
1620	7724	3840	685	6060	212
1680	7218	3900	648	6120	179
1740	6710	3960	633	6180	199
1800	6384	4020	635	6240	160
1860	5992	4080	578	6300	186
1920	5493	4140	536	6360	200
1980	5178	4200	491	6420	201
2040	4882	4260	486	6480	184
2100	4432	4320	496	6540	188
2160	4129	4380	489	6600	192

Shot 6 – NIF System:

Samples Counted	Sample Mass (g)	Distance to DPF (cm)	Counting Order
1 inch #15	41.64	40.48	1
1 inch #22	42.78	40.48	2

Time (s)	Counts	Time(s)	Counts	Time(s)	Counts
0	4	2220	1820		
60	703	2280	1611		
120	18091	2340	1481		
180	16816	2400	1399		
240	15489	2460	1289		
300	14511	2520	1237		
360	13680				
420	12828				
480	11831				
540	11055				
600	10222				
660	9848				
720	8933				
780	327				
840	3				
900	2				
960	4				
1020	3930				
1080	5965				
1140	5639				
1200	4956				
1260	4855				
1320	4611				
1380	4282				
1440	4048				
1500	3666				
1560	3433				
1620	3302				
1680	3080				
1740	2812				
1800	2597				
1860	2422				
1920	2344				
1980	2100				
2040	2000				
2100	1765				
2160	4				

Shot 6 – 3" NaI System:

Samples Counted	Sample Mass (g)	Distance to DPF (cm)	Counting Order
1 inch #22	42.78	40.48	1
1 inch #15	41.64	40.48	2

Time (s)	Counts	Time(s)	Counts	Time(s)	Counts
0	54	2280	995	4560	117
60	2	2340	898	4620	115
120	1	2400	830	4680	112
180	3	2460	786	4740	85
240	619	2520	718	4800	86
300	9911	2580	693	4860	77
360	9050	2640	612	4920	82
420	8659	2700	595	4980	92
480	8127	2760	569	5040	75
540	7509	2820	530	5100	66
600	6910	2880	479	5160	86
660	6515	2940	536	5220	71
720	6021	3000	432	5280	76
780	5642	3060	415	5340	58
840	5208	3120	414	5400	56
900	2619	3180	388	5460	66
960	4506	3240	346	5520	73
1020	4038	3300	306	5580	70
1080	3911	3360	298	5640	71
1140	3646	3420	281	5700	68
1200	3292	3480	301	5760	53
1260	3130	3540	286	5820	75
1320	2882	3600	218	5880	46
1380	2630	3660	242	5940	68
1440	2520	3720	233	6000	55
1500	2418	3780	189	6060	56
1560	2193	3840	187	6120	60
1620	2002	3900	170	6180	56
1680	1919	3960	201	6240	52
1740	1860	4020	166	6300	55
1800	1715	4080	147	6360	56
1860	1542	4140	165	6420	66
1920	1395	4200	144	6480	58
1980	1381	4260	133	6540	59
2040	1234	4320	131	6600	67
2100	1192	4380	114	6660	55
2160	1123	4440	137	6720	69
2220	1044	4500	99	6780	44

Time (s)	Counts	Time(s)	Counts	Time(s)	Counts
6840	57				
6900	55				
6960	56				
7020	54				
7080	46				
7140	47				
7200	51				
7260	39				
7320	56				
7380	48				
7440	35				
7500	47				
7560	47				
7620	44				
7680	59				
7740	49				
7800	57				
7860	44				
7920	34				
7980	40				

Shot 8 – NIF System:

Samples Counted	Sample Mass (g)	Distance to DPF (cm)	Counting Order
3 inch #N	384.4	44.29	1
1 inch #4	41.76	44.29	2

Time (s)	Counts	Time(s)	Counts	Time(s)	Counts
0	4	2220	935		
60	4				
120	4				
180	38997				
240	70130				
300	64700				
360	60285				
420	55717				
480	51609				
540	47107				
600	43723				
660	40867				
720	37529				
780	34892				
840	32251				
900	30387				
960	4482				
1020	3629				
1080	3475				
1140	3156				
1200	2983				
1260	2864				
1320	2576				
1380	2437				
1440	2169				
1500	2070				
1560	1972				
1620	1886				
1680	1685				
1740	1622				
1800	1478				
1860	1366				
1920	1392				
1980	1269				
2040	1123				
2100	1048				
2160	1004				

Shot 8 – NSTec System:

Samples Counted	Sample Mass (g)	Distance to DPF (cm)	Counting Order
1 inch #4	41.76	44.29	1
3 inch #N	384.4	44.29	2

Time (s)	Counts	Time(s)	Counts	Time(s)	Counts
0	2	2280	7771	4560	857
60	3	2340	7232	4620	819
120	3	2400	6854	4680	791
180	5743	2460	6362	4740	749
240	11539	2520	5865	4800	738
300	10775	2580	5579	4860	674
360	10147	2640	5286	4920	654
420	9344	2700	4874	4980	690
480	8693	2760	4672	5040	614
540	8195	2820	4343	5100	617
600	7505	2880	3896	5160	588
660	6943	2940	3809	5220	616
720	6660	3000	3579	5280	570
780	6229	3060	3306	5340	538
840	5722	3120	3064	5400	517
900	659	3180	2944	5460	562
960	1	3240	2753	5520	535
1020	23679	3300	2578	5580	480
1080	30814	3360	2391	5640	480
1140	28716	3420	2219	5700	484
1200	27010	3480	2161	5760	507
1260	25155	3540	2090	5820	482
1320	23501	3600	1878	5880	463
1380	21775	3660	1794	5940	462
1440	20661	3720	1677	6000	436
1500	19140	3780	1657	6060	451
1560	17841	3840	1532	6120	403
1620	16453	3900	1434	6180	402
1680	15737	3960	1346	6240	433
1740	14243	4020	1276	6300	432
1800	13858	4080	1249	6360	418
1860	12510	4140	1169	6420	377
1920	11773	4200	1201	6480	407
1980	10871	4260	1079	6540	417
2040	10229	4320	957	6600	402
2100	9578	4380	972	6660	404
2160	9080	4440	846	6720	422
2220	8277	4500	923	6780	407

Time (s)	Counts	Time(s)	Counts	Time(s)	Counts
6840	393	9480	327	12120	306
6900	406	9540	383	12180	316
6960	342	9600	361	12240	329
7020	368	9660	354	12300	303
7080	383	9720	328	12360	320
7140	372	9780	347	12420	309
7200	359	9840	332	12480	305
7260	411	9900	333	12540	294
7320	346	9960	336	12600	311
7380	345	10020	337	12660	305
7440	382	10080	309	12720	294
7500	367	10140	316	12780	329
7560	390	10200	355	12840	300
7620	339	10260	323	12900	281
7680	351	10320	358	12960	337
7740	360	10380	329	13020	312
7800	346	10440	329	13080	306
7860	353	10500	336	13140	338
7920	359	10560	345	13200	317
7980	337	10620	317	13260	314
8040	334	10680	380	13320	324
8100	348	10740	313	13380	312
8160	382	10800	336	13440	345
8220	374	10860	348	13500	291
8280	354	10920	342	13560	296
8340	327	10980	315	13620	314
8400	323	11040	322	13680	310
8460	338	11100	344	13740	322
8520	322	11160	346	13800	300
8580	337	11220	308	13860	330
8640	340	11280	333	13920	333
8700	323	11340	322	13980	306
8760	351	11400	320	14040	291
8820	359	11460	305	14100	320
8880	343	11520	353	14160	322
8940	315	11580	313	14220	344
9000	313	11640	335	14280	329
9060	362	11700	338	14340	321
9120	315	11760	308	14400	322
9180	348	11820	354	14460	341
9240	318	11880	320	14520	315
9300	342	11940	314	14580	293
9360	340	12000	290	14640	287
9420	355	12060	342	14700	296

Time (s)	Counts	Time(s)	Counts	Time(s)	Counts
14760	296	17400	291	20040	286
14820	286	17460	262	20100	309
14880	294	17520	303	20160	262
14940	295	17580	283	20220	260
15000	305	17640	296	20280	282
15060	321	17700	304	20340	268
15120	292	17760	303	20400	289
15180	336	17820	292	20460	271
15240	323	17880	286	20520	295
15300	318	17940	289	20580	263
15360	275	18000	315	20640	274
15420	318	18060	295	20700	255
15480	308	18120	293	20760	279
15540	323	18180	311	20820	314
15600	317	18240	308	20880	276
15660	296	18300	313	20940	271
15720	287	18360	288	21000	322
15780	314	18420	312	21060	277
15840	317	18480	306	21120	275
15900	319	18540	294	21180	288
15960	296	18600	246	21240	279
16020	342	18660	254	21300	310
16080	301	18720	290	21360	277
16140	313	18780	293	21420	291
16200	312	18840	299	21480	258
16260	285	18900	308	21540	270
16320	294	18960	304	21600	249
16380	326	19020	289	21660	292
16440	333	19080	299	21720	284
16500	273	19140	277	21780	276
16560	277	19200	267	21840	282
16620	289	19260	268	21900	276
16680	309	19320	326	21960	291
16740	329	19380	302	22020	259
16800	276	19440	284	22080	262
16860	302	19500	297	22140	261
16920	324	19560	293	22200	271
16980	287	19620	302	22260	299
17040	312	19680	288	22320	273
17100	279	19740	304	22380	283
17160	312	19800	282	22440	281
17220	300	19860	281	22500	238
17280	300	19920	302	22560	273
17340	316	19980	260	22620	298

Time (s)	Counts	Time(s)	Counts	Time(s)	Counts
22680	275	25320	288	27960	272
22740	270	25380	240	28020	222
22800	277	25440	301	28080	258
22860	249	25500	254	28140	258
22920	251	25560	253	28200	263
22980	263	25620	274	28260	259
23040	272	25680	249	28320	243
23100	241	25740	292	28380	225
23160	287	25800	235	28440	273
23220	254	25860	281	28500	254
23280	261	25920	284	28560	251
23340	254	25980	255	28620	225
23400	268	26040	246	28680	262
23460	277	26100	297	28740	244
23520	265	26160	282	28800	226
23580	282	26220	256	28860	262
23640	239	26280	271	28920	273
23700	278	26340	285	28980	278
23760	274	26400	240	29040	248
23820	240	26460	241	29100	234
23880	271	26520	264	29160	237
23940	264	26580	265	29220	262
24000	257	26640	251	29280	264
24060	258	26700	259	29340	248
24120	263	26760	245	29400	256
24180	262	26820	248	29460	252
24240	265	26880	248	29520	272
24300	282	26940	244	29580	235
24360	257	27000	276	29640	250
24420	250	27060	278	29700	237
24480	257	27120	301	29760	212
24540	285	27180	241	29820	228
24600	265	27240	241	29880	246
24660	235	27300	238	29940	257
24720	260	27360	258	30000	236
24780	240	27420	259	30060	258
24840	309	27480	237	30120	236
24900	267	27540	255	30180	237
24960	257	27600	236	30240	241
25020	242	27660	264	30300	235
25080	300	27720	255	30360	236
25140	249	27780	262	30420	245
25200	238	27840	242	30480	267
25260	289	27900	269	30540	271

Shot 9 – NIF System:

Samples Counted	Sample Mass (g)	Distance to DPF (cm)
3 inch #G	384.26	312

Time (s)	Counts	Time(s)	Counts	Time(s)	Counts
0	5	2340	367	4680	83
60	1	2400	284	4740	88
120	1	2460	296	4800	91
180	1	2520	264	4860	94
240	2435	2580	253	4920	78
300	2494	2640	233	4980	92
360	2428	2700	224	5040	74
420	2456	2760	219	5100	77
480	2302	2820	187	5160	77
540	2050	2880	217	5220	79
600	1967	2940	171	5280	93
660	1847	3000	208	5340	68
720	1764	3060	171	5400	81
780	1599	3120	163	5460	73
840	1529	3180	157	5520	74
900	1367	3240	156	5580	77
960	1311	3300	145	5640	90
1020	1210	3360	152	5700	79
1080	1223	3420	131	5760	77
1140	1103	3480	155	5820	74
1200	1024	3540	134	5880	71
1260	960	3600	129	5940	72
1320	905	3660	110	6000	86
1380	843	3720	135	6060	70
1440	740	3780	138	6120	82
1500	726	3840	95	6180	79
1560	744	3900	107	6240	75
1620	649	3960	101	6300	77
1680	550	4020	106	6360	68
1740	577	4080	90	6420	77
1800	527	4140	100	6480	72
1860	525	4200	109	6540	78
1920	500	4260	102	6600	81
1980	481	4320	113	6660	81
2040	425	4380	81	6720	71
2100	453	4440	100	6780	72
2160	402	4500	98	6840	64
2220	367	4560	106	6900	77
2280	335	4620	87	6960	70

Time (s)	Counts	Time(s)	Counts	Time(s)	Counts
7020	64	9660	69	12300	49
7080	73	9720	72	12360	63
7140	66	9780	67	12420	76
7200	76	9840	74	12480	62
7260	69	9900	74	12540	70
7320	72	9960	64	12600	75
7380	69	10020	70	12660	70
7440	70	10080	72	12720	63
7500	73	10140	72	12780	65
7560	72	10200	68	12840	67
7620	78	10260	53	12900	56
7680	66	10320	82	12960	49
7740	77	10380	60	13020	74
7800	68	10440	80	13080	73
7860	68	10500	85	13140	51
7920	81	10560	67	13200	69
7980	71	10620	77	13260	65
8040	66	10680	71	13320	69
8100	73	10740	58	13380	84
8160	63	10800	64	13440	72
8220	73	10860	57	13500	63
8280	71	10920	59	13560	47
8340	59	10980	73	13620	59
8400	60	11040	67	13680	60
8460	72	11100	58	13740	59
8520	63	11160	80	13800	74
8580	67	11220	82	13860	82
8640	68	11280	74	13920	59
8700	91	11340	73	13980	64
8760	66	11400	75	14040	72
8820	69	11460	61	14100	73
8880	65	11520	68	14160	72
8940	75	11580	63	14220	50
9000	79	11640	65	14280	55
9060	65	11700	72	14340	57
9120	71	11760	72	14400	70
9180	65	11820	58	14460	64
9240	71	11880	65	14520	64
9300	66	11940	64	14580	71
9360	59	12000	57	14640	69
9420	59	12060	56	14700	62
9480	76	12120	61	14760	65
9540	76	12180	76	14820	64
9600	70	12240	80	14880	57

Time (s)	Counts	Time(s)	Counts	Time(s)	Counts
14940	73	17580	66	20220	55
15000	80	17640	66	20280	66
15060	60	17700	65	20340	54
15120	44	17760	79	20400	59
15180	60	17820	57	20460	49
15240	61	17880	81	20520	56
15300	45	17940	49	20580	61
15360	71	18000	64	20640	64
15420	54	18060	72	20700	57
15480	66	18120	71	20760	68
15540	61	18180	57	20820	51
15600	63	18240	56	20880	71
15660	71	18300	63	20940	56
15720	67	18360	59	21000	67
15780	61	18420	56	21060	49
15840	52	18480	69	21120	43
15900	58	18540	78	21180	62
15960	55	18600	61	21240	70
16020	58	18660	70	21300	61
16080	39	18720	52	21360	68
16140	65	18780	45	21420	55
16200	49	18840	48	21480	56
16260	63	18900	72	21540	55
16320	61	18960	65	21600	60
16380	55	19020	41	21660	67
16440	62	19080	51	21720	65
16500	59	19140	47	21780	59
16560	74	19200	76	21840	65
16620	60	19260	49	21900	55
16680	69	19320	61	21960	54
16740	55	19380	71	22020	61
16800	63	19440	58	22080	60
16860	45	19500	50	22140	58
16920	64	19560	66	22200	51
16980	59	19620	63	22260	58
17040	63	19680	79	22320	53
17100	62	19740	57	22380	60
17160	62	19800	50	22440	54
17220	49	19860	58	22500	52
17280	70	19920	69	22560	43
17340	61	19980	64	22620	58
17400	53	20040	65	22680	50
17460	67	20100	44	22740	54
17520	53	20160	53	22800	65

Shot 10 – NIF System:

Samples Counted	Sample Mass (g)	Distance to DPF (cm)	Counting Order
1 cm #8	6.34	39.39	1
3 inch #77	383.9	469.1	2

Time (s)	Counts	Time(s)	Counts	Time(s)	Counts
0	3	2220	94		
60	3	2280	88		
120	3	2340	88		
180	2793	2400	74		
240	2865	2460	71		
300	2622	2520	78		
360	2414	2580	56		
420	2196	2640	67		
480	2044	2700	78		
540	1982	2760	54		
600	1814	2820	55		
660	1684	2880	50		
720	1535	2940	47		
780	1511	3000	48		
840	1400	3060	41		
900	1163	3120	36		
960	2	3180	39		
1020	6	3240	36		
1080	233	3300	32		
1140	331	3360	31		
1200	291	3420	32		
1260	281	3480	27		
1320	272				
1380	245				
1440	224				
1500	215				
1560	210				
1620	178				
1680	169				
1740	167				
1800	140				
1860	134				
1920	137				
1980	137				
2040	136				
2100	103				
2160	122				

Shot 10 – NSTec System:

Samples Counted	Length	Distance to DPF (cm)
Rabbit Tube	7.62 cm	40.02

The Rabbit Tube consists of six 1 inch diameter samples stacked back to back in a sheath with ¼" sides for the casing

Time (s)	Counts	Time(s)	Counts	Time(s)	Counts
0	1	2160	6145	4320	745
60	2	2220	5729	4380	674
120	3	2280	5348	4440	590
180	25866	2340	4913	4500	638
240	55940	2400	4484	4560	687
300	52114	2460	4307	4620	590
360	48151	2520	3993	4680	548
420	45149	2580	3721	4740	510
480	42305	2640	3575	4800	540
540	39492	2700	3303	4860	537
600	36344	2760	3107	4920	480
660	34314	2820	2834	4980	477
720	31621	2880	2762	5040	432
780	29270	2940	2526	5100	474
840	27734	3000	2355	5160	458
900	25686	3060	2329	5220	455
960	23771	3120	2223	5280	420
1020	22033	3180	1952	5340	416
1080	20638	3240	1935	5400	432
1140	19277	3300	1768	5460	369
1200	17936	3360	1616	5520	375
1260	16660	3420	1560	5580	362
1320	15757	3480	1447	5640	346
1380	14235	3540	1377	5700	413
1440	13414	3600	1343	5760	375
1500	12598	3660	1263	5820	311
1560	11692	3720	1184	5880	333
1620	11172	3780	1079	5940	381
1680	10362	3840	1085	6000	353
1740	9744	3900	974	6060	343
1800	9157	3960	1007	6120	298
1860	8399	4020	892	6180	322
1920	7894	4080	855	6240	301
1980	7349	4140	788	6300	316
2040	6997	4200	728	6360	341
2100	6447	4260	673	6420	318

Time (s)	Counts	Time(s)	Counts	Time(s)	Counts
6480	341	9120	241		
6540	312	9180	261		
6600	283	9240	256		
6660	298	9300	279		
6720	285	9360	266		
6780	282	9420	283		
6840	282	9480	272		
6900	284	9540	279		
6960	298	9600	266		
7020	299	9660	264		
7080	263	9720	258		
7140	282	9780	252		
7200	270	9840	229		
7260	290	9900	257		
7320	267	9960	249		
7380	277	10020	233		
7440	282	10080	227		
7500	278	10140	263		
7560	271	10200	239		
7620	277	10260	237		
7680	293	10320	244		
7740	272	10380	265		
7800	278	10440	244		
7860	299	10500	251		
7920	263	10560	252		
7980	289	10620	249		
8040	278	10680	264		
8100	242	10740	260		
8160	248	10800	242		
8220	260	10860	263		
8280	250	10920	208		
8340	284	10980	261		
8400	247	11040	245		
8460	262	11100	244		
8520	246	11160	244		
8580	270				
8640	296				
8700	263				
8760	283				
8820	234				
8880	244				
8940	256				
9000	258				
9060	249				

Shot 11 – NIF System:

Samples Counted	Sample Mass (g)	Distance to DPF (cm)	Counting Order
3 inch #4	387.5	98.06	1
1 cm #12	6.3	98.06	2

Time (s)	Counts	Time (s)	Counts	Time (s)	Counts
0	3				
60	2				
120	4				
180	23322				
240	23413				
300	21562				
360	20182				
420	18801				
480	17447				
540	16468				
600	15216				
660	14250				
720	13141				
780	9282				
840	167				
900	249				
960	230				
1020	231				
1080	198				
1140	196				
1200	181				
1260	163				
1320	156				
1380	147				
1440	113				
1500	127				
1560	119				
1620	94				
1680	100				
1740	102				
1800	89				
1860	93				
1920	88				
1980	73				
2040	79				
2100	76				
2160	63				

Shot 11 – 3" NaI System:

Samples Counted	Sample Mass (g)	Distance to DPF (cm)	Counting Order
1 cm #12	6.3	98.06	1
3 inch #4	387.5	98.06	2

Time (s)	Counts	Time (s)	Counts	Time (s)	Counts
0	3	2220	771	4440	123
60	1	2280	729	4500	114
120	111	2340	654	4560	128
180	369	2400	647	4620	108
240	326	2460	622	4680	105
300	313	2520	556	4740	134
360	289	2580	536	4800	90
420	302	2640	511	4860	94
480	277	2700	499	4920	84
540	239	2760	453	4980	90
600	225	2820	411	5040	97
660	206	2880	383	5100	88
720	187	2940	375	5160	102
780	17	3000	339	5220	82
840	2017	3060	360	5280	85
900	3475	3120	341	5340	86
960	3333	3180	297	5400	85
1020	3075	3240	278	5460	89
1080	2895	3300	280	5520	95
1140	2725	3360	240	5580	97
1200	2453	3420	236	5640	82
1260	2409	3480	238	5700	68
1320	2209	3540	208	5760	81
1380	2128	3600	235	5820	83
1440	1931	3660	183	5880	84
1500	1737	3720	180	5940	82
1560	1579	3780	188	6000	67
1620	1543	3840	165	6060	86
1680	1497	3900	170		
1740	1317	3960	147		
1800	1262	4020	132		
1860	1221	4080	157		
1920	1099	4140	145		
1980	1060	4200	124		
2040	933	4260	134		
2100	936	4320	117		
2160	874	4380	114		